

# Non-protein amino acids identified in carbon-rich Hayabusa particles

Eric T. PARKER <sup>\*</sup>1, Queenie H. S. CHAN <sup>2,3</sup>, Daniel P. GLAVIN <sup>1</sup>, and  
Jason P. DWORKIN <sup>1</sup>

<sup>1</sup>Astrobiology Analytical Laboratory, Solar System Exploration Division, NASA Goddard Space Flight Center, Greenbelt, Maryland 20771, USA

<sup>2</sup>Department of Earth Sciences, Royal Holloway University of London, Egham, Surrey TW20 0EX, UK

<sup>3</sup>School of Physical Sciences, The Open University, Walton Hall, Milton Keynes MK7 6AA, UK

\*Corresponding author. E-mail: eric.t.parker@nasa.gov

(Received 27 May 2021; revision accepted 02 February 2022)

**Abstract**—Amino acid abundances in acid-hydrolyzed hot water extracts of gold foils containing five Category 3 (carbon-rich) Hayabusa particles were studied using liquid chromatography with tandem fluorescence and accurate mass detection. Initial particle analyses using field emission scanning electron microscopy with energy-dispersive X-ray spectrometry indicated that the particles were composed mainly of carbon. Prior to amino acid analysis, infrared and Raman microspectroscopy showed some grains possessed primitive organic carbon. Although trace terrestrial contamination, namely L-protein amino acids, was observed in all Hayabusa extracts, several terrestrially uncommon non-protein amino acids were also identified. Some Hayabusa particles contained racemic (D≈L) mixtures of the non-protein amino acids β-aminoisobutyric acid (β-AIB) and β-amino-*n*-butyric acid (β-ABA) at low abundances ranging from 0.09 to 0.31 nmol g<sup>−1</sup>. Larger abundances of the non-protein amino acid β-alanine (9.2 nmol g<sup>−1</sup>, ≈4.5 times greater than background levels) were measured in an extract of three Hayabusa particles. This β-alanine abundance was ≈6 times higher than that measured in an extract of a CM2 Murchison grain processed in parallel. The comparatively high β-alanine abundance is surprising as asteroid Itokawa is similar to amino acid-poor LL ordinary chondrites. Elevated β-alanine abundances and racemic β-AIB and β-ABA in Hayabusa grains suggested these compounds have non-biological and plausibly non-terrestrial origins. These results are the first evidence of plausibly extraterrestrial amino acids in asteroid material from a sample-return mission and demonstrate the capabilities of the analytical protocols used to study asteroid Ryugu and Bennu samples returned by the JAXA Hayabusa2 and NASA OSIRIS-REx missions, respectively.

## INTRODUCTION

Small primitive bodies, including asteroids and comets, are composed of chemical constituents from the early solar system and offer a glimpse at the prebiotic chemical inventory of the planets at or near the time of the origin of life. The delivery of organics by asteroids, comets, and their fragments to the early Earth and other planetary bodies may have been an important source of the chemical ingredients required for life (Chyba & Sagan, 1992).

The soluble organic composition of carbonaceous chondrites (CCs) has been thoroughly investigated and a variety of organic compound classes have been found, including amino acids, amines, alcohols, aldehydes, ketones, polyols, and carboxylic acids (Burton, Stern, et al., 2012; Cronin et al., 1981; Ehrenfreund et al., 2001; Glavin et al., 2020; Kvenvolden et al., 1970; Pizzarello et al., 2004; Simkus et al., 2019). In particular, amino acids are prime targets in organic analyses of extraterrestrial materials because (1) amino acids are the monomers of proteins and may have been key to the

chemical evolution that led to the origin of life; (2) they are frequently found in a range of extraterrestrial samples, including various classes of meteorites and comet-exposed Stardust samples (Elsila et al., 2009, 2016, 2021); (3) the abundances, relative distributions, and enantiomeric and isotopic compositions of amino acids can be precisely measured to help establish the formation mechanisms and origins of these compounds (Simkus et al., 2019); and (4) there is sufficient structural diversity to probe parent body chemistry (Peltzer et al., 1984).

To illustrate (4) above, complex and diverse amino acid distributions can be indicative of asteroidal origins and exposure to parent body aqueous alteration (Aponte et al., 2015; Glavin et al., 2011). In contrast, cometary materials that may not have been exposed to extensive parent body aqueous alteration have so far revealed a much simpler amino acid distribution of glycine and possibly  $\beta$ -alanine ( $\beta$ -Ala; Altwegg et al., 2016; Elsila et al., 2009). Moreover, it has been shown that an amino acid distribution enriched in  $n$ - $\omega$ -amino acids (straight-chain, terminal amine) is often observed in meteorites that have experienced significant parent body thermal alteration (Burton, Elsila, et al., 2012; Burton et al., 2015). Furthermore, examining enantiomeric and isotopic compositions of amino acids in carbonaceous chondrites has revealed, in select cases, evidence of non-terrestrial L-enantiomeric excesses ( $L_{ee}$ ) for some amino acids, providing important insights into the plausibility of abiotic chiral symmetry breaking mechanisms and a possible origin of biological homochirality on Earth (Cronin & Pizzarello, 1997; Elsila et al., 2016; Engel & Macko, 1997; Glavin et al., 2020; Glavin & Dworkin, 2009; Pizzarello & Cronin, 2000; Pizzarello et al., 2003). While meteoritic amino acid enantiomeric excesses have been observed in some meteorites, it is worth pointing out that racemic amino acids have also been detected in many meteorites. For example, nearly 50/50 D/L ratios for all tested chiral protein and non-protein amino acids in the Antarctic CM2 Yamato 791191 have been reported (Hamase et al., 2014); however, uncertainty estimates were not provided with these enantiomeric abundance estimates for the purpose of evaluating if the quantitated chiral amino acids were racemic within error. Other examples of the detection of racemic amino acids in various primitive Antarctic CR carbonaceous chondrites have also been reported (Glavin et al., 2011; Glavin & Dworkin, 2009; Martins, Alexander, et al., 2007).

As an alternative to making inferences about environments of unknown parent bodies via the analyses of CC chemical compositions, sample-return missions offer unique opportunities to explore the organic chemistry of known, small solar system bodies that have not been exposed to terrestrial weathering like most, if not all, fallen meteorites (Kvenvolden et al.,

2000). Sample-return missions also enable the analyses of these bodies using laboratory techniques not feasible to include on a spacecraft payload focused on in situ exploration. Despite the distinct advantages of analyzing returned samples, these materials are more challenging to obtain than meteorites, and consequently are typically less abundantly available than CCs.

The Japan Aerospace Exploration Agency (JAXA) Hayabusa mission was the first sample-return mission to collect and return asteroid materials to Earth. Hayabusa was launched in 2003 to near-Earth asteroid 25143 Itokawa, and returned particles to Earth in 2010. These particles were split up into four categories based on the compositions of the particles. For example, Category 2 particles are silicate-containing, while Category 3 particles are carbon-rich (<https://curation.isas.jaxa.jp/curation/hayabusa/>, accessed 22 February 2022).

A variety of research efforts have been undertaken to investigate the chemistry of Hayabusa particles. To illustrate, the chemistry of several Category 3 particles has been explored by others (Naraoka et al., 2015; Uesugi et al., 2014; Yabuta et al., 2014) in an attempt to determine the possible origins of these particles. Numerous microanalytical techniques, including scanning electron microscopy (SEM), nanosecond ion mass spectrometry (NanoSIMS), and time-of-flight secondary ion mass spectrometry (ToF-SIMS), were implemented to study Category 3 particles and observed a combined lack of isotopic anomalies and chemical features different from those of meteoritic insoluble organic matter, suggesting the particles were unlikely to be extraterrestrial (Uesugi et al., 2014). A scanning transmission X-ray microscope using X-ray absorption near edge structure spectroscopy was applied to study additional Category 3 particles, which also resulted in the observation of a lack of isotopic anomalies, indicating the particles were not obviously of extraterrestrial origin (Yabuta et al., 2014). Furthermore, ToF-SIMS analyses identified a homogeneous carbon distribution in Category 3 particles that was seemingly associated with fluorine, nitrogen, and silicon, which is distinct from that observed in carbon-rich extraterrestrial samples, underscoring the possibility the particles were likely to be artifacts (Naraoka et al., 2015). Although these reports suggested contamination was a plausible source of Category 3 particles, neither of these studies were able to conclusively rule out the possibility of extraterrestrial origin, citing such evidence as isotopically normal compounds not being uncommon in extraterrestrial material, including micrometeorites and interplanetary dust particles (Messenger, 2000; Yabuta et al., 2013). Instead, it was emphasized that additional studies of the chemistry of Category 3 particles were needed (Yabuta et al., 2014), which would help to better ascertain the origin of Hayabusa particles.

There has only been one reported effort to explore the amino acid chemistry of Hayabusa particles, however. The amino acid analyses of dichloromethane/methanol extracts of two Category 2 Hayabusa particles (RA-QD02-0033 and RA-QD02-0049) were published in 2012 (Naraoka et al., 2012). The analyses were conducted using a very sensitive two-dimensional high-performance liquid chromatography with fluorescence detection technique that detected only glycine and alanine, but at abundances (glycine = 364 fmol; D,L-alanine = 105 fmol) similar to blank levels (glycine = 231 fmol, D,L-alanine = 76 fmol) with a correspondingly large alanine  $L_{ee}$  of  $\approx 45\%$ , and therefore were attributed to terrestrial contamination (Naraoka et al., 2012). Consequently, to date, it remains unclear if any other Hayabusa particles contain indigenous amino acids.

To address this absence in the literature, we have investigated the amino acid content of five Category 3 Hayabusa particles that have not previously been analyzed for amino acids, along with a grain of the CM2 Murchison meteorite (provided by Dr. Michael Zolensky from the NASA Johnson Space Center and stored in an  $N_2$  cabinet prior to allocation). The assumption that Category 3 particles are the result of contamination is partially what motivated the current work. Since prior investigations (Naraoka et al., 2015; Uesugi et al., 2014; Yabuta et al., 2014) were unable to confirm the origin of Category 3 particles, a logical subsequent step to evaluate the provenance of Category 3 particles is to analyze their amino acid content. In this work, we used ultrahigh-performance liquid chromatography with fluorescence detection and time-of-flight mass spectrometry (LC-FD/ToF-MS) to study the amino acid content of Category 3 particles. The acid-hydrolyzed hot water extracts from these particles were analyzed to maximize the abundance of amino acids and thereby improve the chance of target analyte detection in these tiny samples.

## MATERIALS AND METHODS

### Particle Samples and Controls

Five Hayabusa particles were allocated by the JAXA Planetary Material Sample Curation Facility as part of its distribution for the 3rd International Announcement of Opportunity: RA-QD02-0012, RB-CV-0029, RB-CV-0080, RB-QD04-0052, and RA-QD02-0078 (Fig. 1), referred to as #12, #29, #80, #52, and #78, respectively. The particles, ranging in size from 83 to 100  $\mu m$  in the longest dimension, were selected for the following reasons. (1) All were Category 3 grains (Chan et al., 2021; Ito et al., 2014; Kitajima et al., 2015; Yabuta et al., 2014) based on initial field emission

scanning electron microscopy (FE-SEM) with energy-dispersive X-ray spectrometer (EDX) characterization (Fig. S2 in the supporting information). (2) #80 contained signatures for elemental N, C, and O based on SEM-EDX analysis. (3) The particles were among the largest samples in the Hayabusa Category 3 collection. (4) #52 and #78 showed Raman features consistent with primitive unheated organic matter, which may be more likely to contain amino acids that would otherwise decompose at elevated temperatures (Ratcliff et al., 1974). All Hayabusa samples were kept in glass slides that were sealed inside original sealed JAXA containers that were cleaned as described elsewhere (Yada et al., 2014), and stored in an ISO Class 5 cleanroom at the Open University. Prior to hot water extraction and acid hydrolysis, all samples were pressed into squares of baked gold foil to secure the particles during the execution of sample preparation protocols. A CM2 Murchison grain ( $\approx 200 \mu m$  prior to pressing into gold foil) and a baked gold foil procedural blank were extracted in parallel with the Hayabusa samples. The gold foil procedural blank and all sample handling tools were cleaned by baking at 500  $^{\circ}C$  in air for  $>10$  h prior to use.

Details pertaining to the characteristics of the Hayabusa particles studied here can be found at the JAXA Hayabusa Curation website (<https://curation.isas.jaxa.jp/curation/hayabusa/>, accessed 22 February 2022), but will be briefly overviewed here. Particle #12 contained CO and FeS; #29 is a plagioclase particle composed of (C,O) and sodium chloride; #80 is comprised of (C,N,O), (C,O), aluminum, potassium, and silicone; #52 contains (C,F,O), aluminum, and titanium; and #78 is composed of CO, chloride, CFO, and magnesium. SEM data demonstrating these chemical compositions are shown in Fig. S2.

As both #52 and #78 exhibited clear organic signatures in their Raman spectra (see §1.2 of supporting information for more details), they were estimated to contain higher abundances of organic material on a per-grain basis and thus were pressed into their own respective squares of gold foil to allow for the amino acid analysis of their individual masses. Particles #12, #29, and #80 (referred to as #12,29,80) were all pressed into the same square of gold foil to allow for the amino acid analysis of their combined masses. An explanation for why these three particles were combined prior to analysis is provided in §1.2 of the supporting information. Sample and procedural blank properties are presented in Table 1. Additional details about the sample extraction and preparation procedures, as well as analytical conditions used for LC-FD/ToF-MS detection of amino acids in the samples, can be found in §1.2–1.3 of the supporting information.

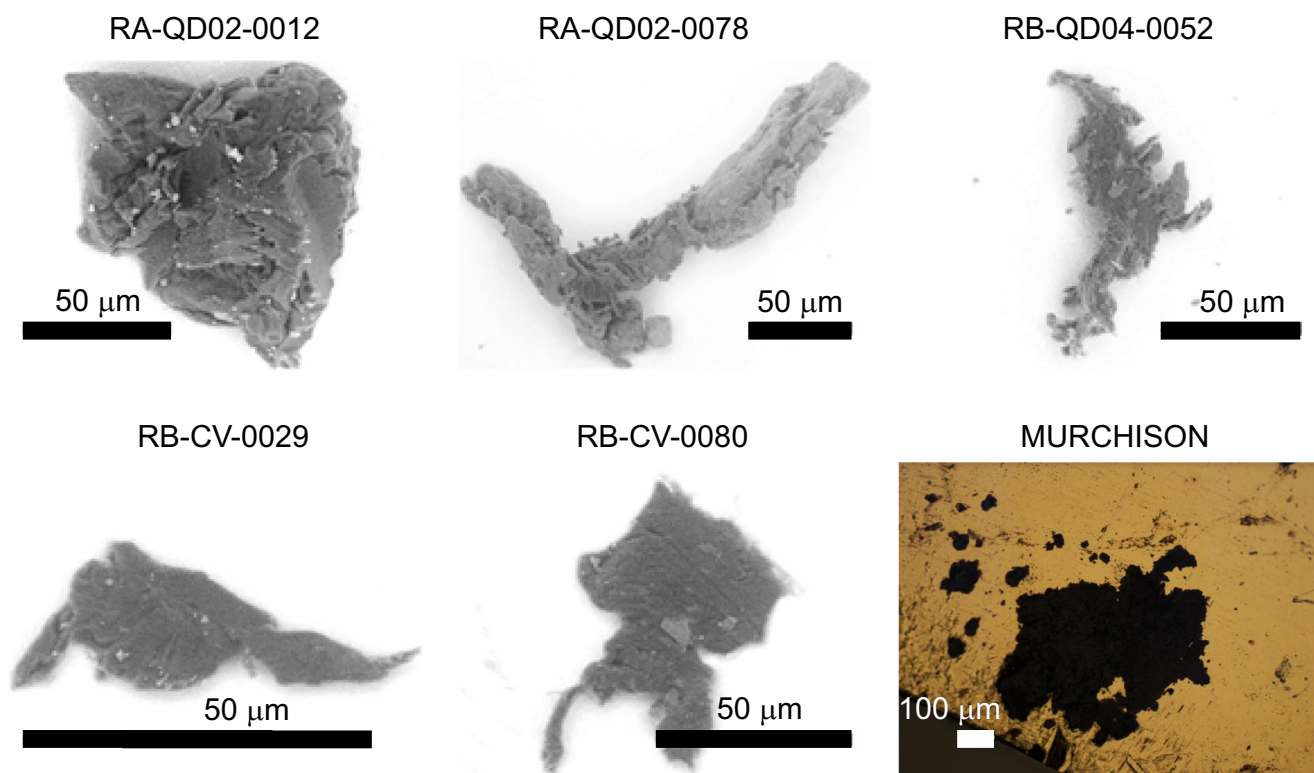


Fig. 1. Images of the five Hayabusa particles and one Murchison grain analyzed in this study. Backscattered electron images of the five allocated Hayabusa particles, obtained by SEM-EDX spectroscopy analysis at the Extraterrestrial Sample Curation Center of JAXA. Also included is a microphotograph of the Murchison grain studied here. In the Murchison grain image, the gold foil the grain has been pressed in is visible in the background.

## RESULTS AND DISCUSSION

### Amino Acid Results

Representative UV fluorescence chromatograms from LC analyses of an amino acid standard mixture, and the gold foil procedural blank, Murchison, and #12,29,80 extracts are shown in Fig. 2. Several peaks observed in the gold foil procedural blank extract that were identified as common amino acid contaminants, including *L*-enantiomers of protein amino acids, were also found in the Murchison and Hayabusa grain extracts, and thus were attributed to terrestrial contamination from the work-up procedure. The most abundant terrestrial contaminant was  $\epsilon$ -amino-*n*-caproic acid ( $\epsilon$ -ACA) (Fig. S5 in the supporting information), the hydrolysis product of nylon 6 and a common material used in clean rooms and laboratories (Dworkin et al., 2018). For more details on this contaminant and possible sources, see §2.2 of the supporting information. It should be emphasized that the presence of terrestrial contamination in the sample extracts did not prevent the detection and quantitation of amino acids at elevated abundances relative to background levels, as

can be seen from the averaged, blank-corrected amino acid abundances reported in Table 2. Despite the primitive organic Raman signatures, #52 and #78 were largely depleted in amino acids, with peaks that were similar in intensity to those of the gold foil procedural blank. More details of the amino acid results for these two Hayabusa samples are provided in §2.2–2.3 of the supporting information. In contrast to #52 and #78, the acid-hydrolyzed hot water extracts of Murchison and #12,29,80 contained a suite of amino acids present at abundances above background levels.

The most prominent examples of amino acid detections that were likely to be indigenous to the samples were those of the non-protein amino acids,  $\alpha$ -aminoisobutyric acid ( $\alpha$ -AIB),  $\beta$ -Ala,  $\beta$ -aminoisobutyric acid ( $\beta$ -AIB),  $\beta$ -amino-*n*-butyric acid ( $\beta$ -ABA), and  $\gamma$ -amino-*n*-butyric acid ( $\gamma$ -ABA). Both #52 and #78 were found to contain a limited amino acid distribution, primarily comprised of low abundances ( $0.123 \pm 0.002$  nmol g<sup>-1</sup> and  $0.030 \pm 0.001$  nmol g<sup>-1</sup>, respectively) of  $\beta$ -AIB. Both Murchison and #12,29,80 contained low abundances of  $\beta$ -AIB ( $0.16 \pm 0.01$  nmol g<sup>-1</sup> and  $0.31 \pm 0.03$  nmol g<sup>-1</sup>, respectively) and  $\beta$ -ABA ( $0.048 \pm 0.001$  nmol g<sup>-1</sup> and  $0.090 \pm 0.005$  nmol g<sup>-1</sup>, respectively).

Table 1. Measured masses of the gold foils and estimated masses of the Hayabusa particles and Murchison grain extracted for amino acid analyses in this study.

Specimens	Mass of gold foil used for each specimen (mg)	Total surface area of each pressed sample ( $\mu\text{m}^2$ )	Estimated masses of pressed samples ( $\mu\text{g}$ ) <sup>a,b</sup>
Gold foil	2.16	N/A	N/A
procedural blank			
Murchison	4.41	238,464	3.82
#12,29,80	3.23	12,805	0.20
#52	2.49	8147	0.13
#78	3.03	21,362	0.34

<sup>a</sup>Masses were estimated based on an assumed flattened sample thickness of  $5\mu\text{m}$  and a specific gravity of  $3.2\text{ g cm}^{-3}$  of the dominant mineral phases (forsterite and enstatite) of Itokawa. Despite these known dominant mineral phases of Itokawa, the dominant mineral phases of the Hayabusa particles studied here were not confirmed prior to analysis. To mitigate potential sample contamination or destruction using common techniques implemented when exploring mineralogy, such as SEM and electron probe microanalysis, the microparticles studied here were dedicated for amino acid analyses only. Consequently, the specific mineralogy of the particles studied here is not known in detail and is thus not thoroughly discussed here.

<sup>b</sup>Mass estimates were obtained by a three-step process. First, direct measurements of grain dimensions for each particle were made on an optical image to obtain the surface area of each pressed particle. Second, a flattened sample thickness of  $5\mu\text{m}$  was assumed and multiplied by the pressed particle surface area to deduce the particle volume. Third, the mass estimates were calculated via multiplying the particle volume by the specific gravity of  $3.2\text{ g cm}^{-3}$ . Consequently, the accuracies of the particle mass estimates are dependent on the accuracies of the measured dimensions of each particle via optical imagery. To this end, the optical images were taken at  $1280 \times 960$  pixels<sup>2</sup> at 20x magnification. At this magnification, the resolution was  $\approx 0.5\mu\text{m pixel}^{-1}$ . Furthermore, the specific gravity of  $3.2\text{ g cm}^{-3}$  has been estimated for LLs (Wilkison & Robinson, 2000). Considering that Itokawa is compositionally similar to LL5 and LL6 chondrites, the specific gravity value used here is consistent with literature findings. In this work, we have also discussed the possibility that the particles might be derived from a C-type parent body, potentially a CR, and the specific gravity of  $3.2\text{ g cm}^{-3}$  is also similar to this range of samples (e.g., Renazzo,  $3.05\text{ g cm}^{-3}$ , Acfer 270,  $3.26\text{ g cm}^{-3}$  [Macke et al., 2011]). Therefore, it remains plausible that the specific gravity values may be lower for some CCs (e.g., Al Rais and some CMs) in which case it is possible the actual masses for Category 3 (carbonaceous) grains could be lower. Under such a scenario, the particle masses given here would likely represent upper limit estimates.

It must be emphasized that neither  $\beta$ -AIB nor  $\beta$ -ABA was identified in the procedural blank (Fig. S7 in the supporting information) and these two non-protein amino acids were present as racemic ( $D \approx L$ ) or nearly racemic mixtures in the Hayabusa and Murchison samples within

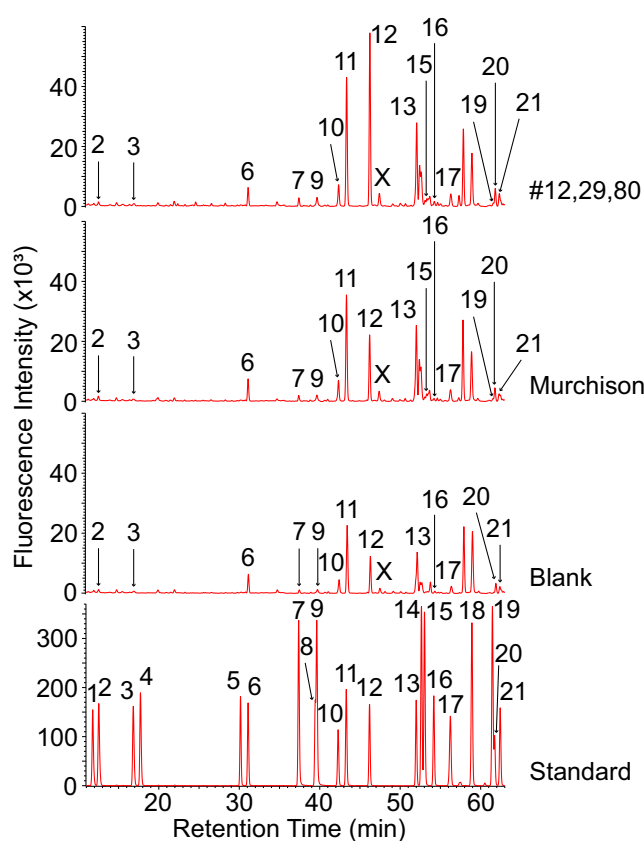


Fig. 2. Although contamination was observed,  $\beta$ -Ala (peak 12) was still found to be markedly larger in the #12,29,80 sample compared to the blank. The 11- to 63-min regions of the fluorescence chromatograms for a mixed amino acid standard, the procedural blank, Murchison, and #12,29,80. Analyte identifications are as follows: 1 = D-aspartic acid (D-Asp), 2 = L-Asp, 3 = L-glutamic acid (L-Glu), 4 = D-Glu, 5 = D-serine (D-Ser), 6 = L-Ser, 7 = D-isoserine (D-Ise), 8 = D-threonine (D-Thr), 9 = L-Ise, 10 = L-Thr, 11 = glycine (Gly), 12 =  $\beta$ -alanine ( $\beta$ -Ala), 13 =  $\gamma$ -amino-*n*-butyric acid ( $\gamma$ -ABA), 14 = D- $\beta$ -aminoisobutyric acid (D- $\beta$ -AIB), 15 = L- $\beta$ -AIB, 16 = D-Ala, 17 = L-Ala, 18 = D- $\beta$ -ABA, 19 = L- $\beta$ -ABA, 20 =  $\delta$ -aminovaleric acid ( $\delta$ -AVA), 21 =  $\alpha$ -AIB. Note: peak X is an unidentified compound with a primary amino group.

analytical errors (Table S4 in the supporting information). Furthermore, it should be stressed that  $\beta$ -AIB and  $\beta$ -ABA are not common in natural samples, but have been detected above background levels in previous analyses of carbon-rich meteorites (Burton et al., 2014). There are select examples, however, of racemic  $\beta$ -ABA having been detected in natural terrestrial samples (Burton et al., 2011, 2014) that were dominated by biology and possibly influenced by industrial contamination. To evaluate the juxtaposition between racemic  $\beta$ -ABA detected in terrestrial samples and the particles analyzed here, it is helpful to compare the abundances of  $\beta$ -ABA relative to other amino acids found in terrestrial samples, with the same relative abundances in the particles analyzed here. In

Table 2. Summary of the averaged, blank-corrected abundances (nmol g<sup>-1</sup>) of the C<sub>2</sub>–C<sub>6</sub> amino acids in the acid-hydrolyzed (total) hot water extracts of the CM2 Murchison and Hayabusa particles analyzed here.

C#	Amine position	Amino acid	Murchison (Glavin et al., 2021), (0.08 g)	Murchison (present work) (3.82 µg)	#12,29,80 (0.20 µg)	#52 (0.13 µg)	#78 (0.34 µg)
2	α	Gly	40 ± 3	1.62 ± 0.04 <sup>a</sup>	3.86 ± 0.05 <sup>a</sup>	n.d.	n.d.
3	α	D-Ala	2.2 ± 0.01	0.03 ± 0.02	0.20 ± 0.06	n.d.	n.d.
3	α	L-Ala	3.0 ± 0.2	0.27 ± 0.02	0.41 ± 0.02	n.d.	n.d.
3	α	D-Ser	0.13 ± 0.03	n.d.	n.d.	n.d.	n.d.
3	α	L-Ser	3.5 ± 0.1	0.21 ± 0.01	n.d.	n.d.	n.d.
3	β	β-Ala	6.0 ± 0.2	1.49 ± 0.05	9.2 ± 0.3	n.d.	n.d.
3	β	D-Ise	N.R.	0.053 ± 0.004 <sup>a</sup>	0.150 ± 0.005 <sup>a</sup>	n.d.	n.d.
3	β	L-Ise	N.R.	0.083 ± 0.003 <sup>a</sup>	0.22 ± 0.01 <sup>a</sup>	n.d.	n.d.
4	α	D-Asp	0.59 ± 0.02	n.d.	n.d.	n.d.	n.d.
4	α	L-Asp	3.0 ± 0.1	0.05 ± 0.01 <sup>b</sup>	0.02 ± 0.01 <sup>b</sup>	n.d.	n.d.
4	α	D-Thr	0.02 ± 0.01	n.d.	n.d.	n.d.	n.d.
4	α	L-Thr	2.21 ± 0.05	0.546 ± 0.005	0.86 ± 0.04	n.d.	n.d.
4	α	D,L-α-ABA	2.0 ± 0.4	n.d.	n.d.	n.d.	n.d.
4	α	α-AIB	11.4 ± 0.5	0.21 ± 0.03	0.10 ± 0.01	n.d.	n.d.
4	β	D-β-ABA	1.8 ± 0.1	0.024 ± 0.001 <sup>c</sup>	0.044 ± 0.005 <sup>c</sup>	n.d.	n.d.
4	β	L-β-ABA	1.6 ± 0.1	0.0246 ± 0.0004 <sup>c</sup>	0.047 ± 0.002 <sup>c</sup>	0.015 ± 0.001 <sup>c</sup>	n.d.
4	β	D-β-AIB	2.4 ± 0.6 <sup>d</sup>	0.085 ± 0.006 <sup>c</sup>	0.16 ± 0.02 <sup>c</sup>	0.062 ± 0.002 <sup>c</sup>	0.0163 ± 0.0006 <sup>c</sup>
4	β	L-β-AIB		0.07 ± 0.01 <sup>c</sup>	0.14 ± 0.02 <sup>c</sup>	0.060 ± 0.001 <sup>c</sup>	0.0137 ± 0.0009 <sup>c</sup>
4	γ	γ-ABA		2.07 ± 0.09	3.2 ± 0.2	n.d.	n.d.
5	α	D-Glu	1.03 ± 0.03	n.d.	n.d.	n.d.	n.d.
5	α	L-Glu	6.3 ± 0.1	0.010 ± 0.001 <sup>b</sup>	0.04 ± 0.02 <sup>b</sup>	n.d.	n.d.
5	α	D-Val	0.55 ± 0.02	n.d.	n.d.	n.d.	n.d.
5	α	L-Val	2.8 ± 0.1	0.51 ± 0.03 <sup>a</sup>	0.69 ± 0.02 <sup>a</sup>	0.06 ± 0.01	0.093 ± 0.005
5	α	D-Iva	10.0 ± 0.5	n.d.	n.d.	n.d.	n.d.
5	α	L-Iva	11.8 ± 0.7	n.d.	n.d.	n.d.	n.d.
5	α	D-Nva	0.1 ± 0.1	n.d.	n.d.	n.d.	n.d.
5	α	L-Nva	0.05 ± 0.03	n.d.	n.d.	n.d.	n.d.
5	β	S-3-APA	2.7 ± 0.1	n.d.	n.d.	n.d.	n.d.
5	β	R-3-APA		n.d.	n.d.	n.d.	n.d.
5	δ	δ-AVA	1.8 ± 0.1	0.39 ± 0.02 <sup>a</sup>	0.96 ± 0.07 <sup>a</sup>	n.d.	n.d.
6	α	D-Leu	N.R.	n.d.	n.d.	n.d.	n.d.
6	α	L-Leu	N.R.	n.d.	n.d.	0.07 ± 0.01 <sup>a</sup>	0.064 ± 0.006
6	α	D-Ile	N.R.	n.d.	n.d.	n.d.	n.d.
6	α	L-Ile	N.R.	n.d.	n.d.	0.021 ± 0.001 <sup>c</sup>	0.0401 ± 0.0002
6	ε	ε-ACA	2.2 ± 0.6	n.d. <sup>c,e</sup>	n.d. <sup>c,e</sup>	n.d. <sup>c,e</sup>	n.d. <sup>c,e</sup>

For comparison, amino acid concentrations measured in the acid-hydrolyzed (total) hot water extract of a 0.08 g Murchison specimen (Glavin et al., 2021) are provided here. All data reported in the table from the current study are based on quantitation via optical fluorescence, except where noted by a superscript in the table (superscript definitions provided below). Blank corrections were performed by controlling for differences in surface areas of gold foils and derivatization volumes used between the procedural blank and the samples (see §1.3.1. of the supporting information for further details). Uncertainties ( $\delta_x$ ) reported here were calculated as the standard error ( $\delta_x = \sigma_x \times (n)^{-1/2}$ ) based on the standard deviation ( $\sigma_x$ ) of the average values of triplicate ( $n = 3$ ) measurements.

n.d. = Not determined because analyte abundance did not exceed blank levels.

N.R. = Analyte abundance not reported.

<sup>a</sup>Target analyte was tentatively detected by retention time and optical fluorescence, compared to an analytical standard. However, unambiguous identification of the target analyte was not confirmed because an unidentified analyte possessed an experimental accurate mass that overlapped with that of the target analyte, causing the measured experimental accurate mass of the target analyte to exceed the 10 parts per million (ppm) mass tolerance used. Consequently, the measurement of the target analyte did not experience interference via optical fluorescence, but did experience interference via accurate mass analysis. Therefore, abundances reported here are based on optical fluorescence and serve as upper limit estimates.

<sup>b</sup>Analyte was detected and quantitated via optical fluorescence, but was not detected by the mass spectrometer, due to inefficient ionization of the analyte in a heavily aqueous eluent composition.

<sup>c</sup>Quantitation of analytes was performed via ToF-MS due to interfering, optically fluorescent species that were fully resolved by accurate mass analysis.

<sup>d</sup>Analyte abundance was reported as the sum of abundances for γ-ABA + D,L-β-AIB because the analytes were not separated under the chromatographic conditions used.

<sup>e</sup>Measured sample ε-ACA abundances were <1.12 nmol, which was observed in the gold foil procedural blank.

<sup>f</sup>Unambiguous identification of the target analyte was not confirmed due to an unidentified analyte that coeluted with the target analyte via optical fluorescence and also possessed an experimental accurate mass that overlapped with that of the target analyte, causing the measured experimental accurate mass of the target analyte to exceed the 10 ppm mass tolerance used. Consequently, quantitation was not performed.



particular, comparing the abundances of  $\beta$ -ABA to common terrestrial contaminants, such as glycine and alanine, can help determine if the  $\beta$ -ABA detected in the particles is likely to have originated from a terrestrial source. To illustrate, if the  $\beta$ -ABA relative abundances in the particles are dissimilar from those of terrestrial samples, such a finding would indicate that the  $\beta$ -ABA detected in the particles is not likely to be the result of terrestrial processes. Although  $\epsilon$ -ACA derived from nylon 6 was the most abundant amino acid contaminant in the Hayabusa sample extracts, nylon 6 does not contain  $\beta$ -ABA (Glavin et al., 2006), so nylon contamination is not a source of the elevated  $\beta$ -ABA in the Hayabusa samples. In addition, amino acid data from four terrestrial samples that can also be used for comparative purposes include soil samples from several meteorite fall sites in Murchison, Australia and Aguas Zarcas, Costa Rica (Glavin et al., 2021); Sutter's Mill, California (Burton et al., 2014); and Almahata Sitta, Sudan (Burton et al., 2011). The  $\beta$ -ABA/Gly ratio for Hayabusa material is  $0.024 \pm 0.001$ , while the same ratios for the Murchison, Aguas Zarcas, Sutter's Mill, and Almahata Sitta soils are  $<0.009$ ,  $0.0025 \pm 0.0002$ ,  $0.004 \pm 0.001$ , and  $0.003 \pm 0.001$ , respectively. Excluding the Murchison soil sample where  $\beta$ -ABA was not detected, the other soils possessed an average  $\beta$ -ABA relative abundance of  $0.0032 \pm 0.0003$ , which is  $>7.5\times$  smaller than the  $\beta$ -ABA relative abundance of the Category 3 particles studied here. Similarly, the  $\beta$ -ABA/Ala ratio for the particles returned by Hayabusa is  $0.15 \pm 0.02$ , whereas the same ratios for the aforementioned soils are  $<0.015$ ,  $0.0038 \pm 0.0004$ ,  $0.003 \pm 0.001$ , and  $0.006 \pm 0.002$ , respectively. This equates to an average  $\beta$ -ABA/Ala ratio for the three terrestrial soils where  $\beta$ -ABA was detected of  $0.0043 \pm 0.0005$ , which is  $\approx 35\times$  smaller than the  $\beta$ -ABA relative abundance of the particles studied here. Consequently, the relative abundances of  $\beta$ -ABA detected in the Hayabusa particles analyzed in the current work are much higher than what is observed in terrestrial samples, suggesting that most of the  $\beta$ -ABA detected in the particles returned by the Hayabusa mission is plausibly extraterrestrial in origin. In the absence of dedicated Hayabusa contamination control witness materials available for amino acid analysis, these soils from four continents are the best available proxies for a range of plausible biological and industrial sources of amino acids. The amino acid analyses of the OSIRIS-REx spacecraft construction did not detect any  $\beta$ -ABA. Instead, the low levels of amino acid contamination were dominated by glycine ( $0.96\text{--}13.1 \text{ ng cm}^{-2}$ ) on different spacecraft surfaces (Dworkin et al., 2018) and were also inconsistent with the  $\beta$ -ABA/Gly ratios observed in the Hayabusa material. These combined observations of natural and industrial amino acid ratios provide additional supporting evidence

to suggest these analytes were not likely to be a result of terrestrial contamination imparted during sample handling.

Regarding additional non-protein amino acids of interest, Murchison had an elevated ( $\approx 2$  times higher than background levels) abundance of  $\gamma$ -ABA, whose total abundance was  $2.07 \pm 0.09 \text{ nmol g}^{-1}$ . Murchison also had an enhanced ( $\approx 3.4$  times higher than background levels) abundance of  $\alpha$ -AIB (total abundance =  $0.21 \pm 0.03 \text{ nmol g}^{-1}$ ). This observation is consistent with previous reports that  $\alpha$ -AIB is among the more abundant non-protein amino acids in Murchison (Cronin & Pizzarello, 1983; Engel & Nagy, 1982; Glavin et al., 2021). The elevated abundances of  $\alpha$ -AIB and  $\gamma$ -ABA in the Murchison grain extract, relative to blank levels (Fig. S11 in the supporting information), are a similar observation to that of a much larger Murchison sample mass that was extracted and analyzed for amino acids (Glavin et al., 2021). Such a similarity provides additional evidence that some portions of  $\alpha$ -AIB and  $\gamma$ -ABA detected in the Murchison grain extract were likely derived from the particle itself. It is also worth noting that  $\delta$ -aminovaleric acid ( $\delta$ -AVA) was tentatively identified in the acid-hydrolyzed hot water extract of Murchison and #12,29,80, at lower abundances than other  $n$ - $\omega$ -amino acids (Table 2), similar to that observed in the analyses of larger quantities of Murchison (Glavin et al., 2021). It should be emphasized that such comparisons made here were done primarily for initial screening purposes, as opposed to verifying the absolute veracity of the amino acid abundances in the Murchison grain. To illustrate, comparing the analyses of a particle of Murchison to those of much larger samples of Murchison was executed simply to determine if the amino acid abundances and distributions observed in the Murchison particle were at all consistent with what would be expected of a Murchison sample based on previous literature reports. If not, this would indicate that the particle analyses performed here may not properly capture the amino acid content of the sample. However, since the comparison between the analytical results of the Murchison particle and that of larger Murchison samples was similar to a first approximation, this observation provided an indication that the particle analyses performed here were accurate and reliable.

Perhaps the most intriguing amino acid detection example in this work was that of  $\beta$ -Ala for #12,29,80 where  $\beta$ -Ala was  $\approx 4.5$  times more abundant than blank levels (Fig. 3), with a total abundance of  $9.2 \pm 0.3 \text{ nmol g}^{-1}$ . To help evaluate the possibility that some of the  $\beta$ -Ala observed in the #12,29,80 extract may be of extraterrestrial origin, it is useful to compare the abundances of  $\beta$ -Ala in the sample and the blank,

relative to a common terrestrial protein amino acid contaminant, like alanine (Fig. 4). This comparison shows that the #12,29,80  $\beta$ -Ala relative abundance is  $\approx 2.5$  times greater than that observed for the blank, and is thus sufficiently distinct from background levels to indicate that the presence of  $\beta$ -Ala in #12,29,80 is not due to contamination sources alone. To further assess the possibility that  $\beta$ -Ala may have originated from terrestrial sources, it is worth comparing the relative abundance of  $\beta$ -Ala to that of aspartic acid, a common terrestrial amino acid. To explain, it has previously been reported that  $\beta$ -Ala can be produced by the  $\alpha$ -decarboxylation of aspartic acid (Peterson et al., 1997), and that another non-protein amino acid,  $\gamma$ -ABA, can be formed by the hydrolysis of 2-pyrrolidone, the pyrolysis product of glutamic acid (Lie et al., 2018; Vallentyne, 1964; Weiss et al., 2018). Thus, comparing the abundance of  $\beta$ -Ala relative to  $\gamma$ -ABA, to the abundance of aspartic acid relative to glutamic acid, can provide insight into the plausibility that the enlarged  $\beta$ -Ala abundance observed here may have been due to terrestrial amino acid contamination and subsequent degradation. For the #12,29,80 sample, the  $\beta$ -Ala/ $\gamma$ -ABA ratio is  $2.9 \pm 0.2$  and the Asp/Glu ratio is  $0.5 \pm 0.4$ . If these two ratios were similar to each other, that would suggest  $\beta$ -Ala was likely derived from aspartic acid. However, since these two ratios are clearly distinct from one another, this finding indicates that the elevated levels of  $\beta$ -Ala in the #12,29,80 sample are unlikely to be caused by the degradation of common terrestrial contaminant amino acids like aspartic acid, alone. Therefore, the combination of four different and consistent abundance characteristics associated with  $\beta$ -Ala in the #12,29,80 sample indicated that a portion of the  $\beta$ -Ala in the acid-hydrolyzed hot water extract must have been derived from the sample itself, and not contamination from the processing procedures. These characteristics include (1) enhanced total abundance, (2) enlarged abundance relative to blank levels, (3) heightened relative abundances compared to common terrestrial contaminants (e.g., glycine [Fig. S12 in the supporting information] and alanine [Figs. 4, S13, and S14]), and (4) distinct relative abundance compared to that of aspartic acid, a potential terrestrial source of  $\beta$ -Ala.

In addition to measuring amino acid concentrations and relative abundances, enantiomeric ratios and  $L_{ee}$  of select chiral amino acids were also determined (Table S4). As noted previously,  $\beta$ -ABA was racemic for Murchison and the #12,29,80 grains, as was  $\beta$ -AIB for #12,29,80 and #52 (Table S4). However,  $\beta$ -AIB was found to be slightly enriched in the D-enantiomer for the Murchison grain ( $L_{ee} = -7.5 \pm 7.0\%$ ) and #78 ( $L_{ee} = -8.7 \pm 4.2\%$ ) as indicated by their negative L-enantiomeric excess percentage values that lie just

outside of analytical errors (Table S4). Similar, comparatively large abundance estimates of D- $\beta$ -AIB versus L- $\beta$ -AIB were reported for Murchison by Koga and Naraoka (2017), although these abundance estimates were accompanied by significant uncertainty estimates due to chromatographic interference that was observed. Nonetheless, given the very low concentrations of  $\beta$ -AIB in these Murchison and Hayabusa grain extracts, and their associated relatively large %  $L_{ee}$  uncertainties, the small D- $\beta$ -AIB enantiomeric excesses should be interpreted with caution. Similarly, enantiomeric measurements of isoserine (Ise) for Murchison and #12,29,80 appeared to possess relatively large  $L_{ee}$  values of  $\approx 20\%$  (Table S4), yet it is important to bear in mind that Ise was only tentatively observed at low abundances, which warrants cautious evaluation of Ise enantiomeric excesses as well. Compound-specific stable isotope measurements (Elsila et al., 2009) of the individual D- and L-enantiomers are necessary to firmly establish a non-terrestrial origin of any measured enantiomeric excess. However, due to limited sample mass and low amino acid abundances, isotopic measurements were not feasible here. Future improvements in compound-specific stable isotope measurement technologies for amino acids will be needed to more rigorously evaluate the source of the enantiomeric excesses in these samples.

### Comparison to Previous Itokawa Analyses

Naraoka et al. (2012) reported on the amino acid analyses of two Itokawa particles, which revealed that only glycine and D,L-alanine were detected in the procedural blanks and each of the grains. Extracts of RA-QD02-0033 showed glycine and alanine did not exceed blank levels and RA-QD02-0049 contained low levels of glycine, D-alanine, and L-alanine slightly greater than those observed for the procedural blanks ( $\approx 1.6$ ,  $\approx 1.3$ , and  $\approx 1.4$  times higher, respectively, than blank levels). Reasonably, it was concluded that glycine and D,L-alanine were largely due to contamination (Naraoka et al., 2012). In the current study, however, we observed a much broader distribution of amino acids in the Hayabusa grain extracts, including two terrestrially rare non-protein amino acids that are not common terrestrial contaminants.

The contrast in amino acid results between the present work and Naraoka et al. may be because the Category 3 particles analyzed here were carbon-rich and contained more organic material than the Category 2 particles analyzed by Naraoka et al. (2012). It is also possible that the dissimilar amino acid results might partially be due to differences in sample preparation protocols. Hot water extraction at 100 °C for 24 h was used in this study,



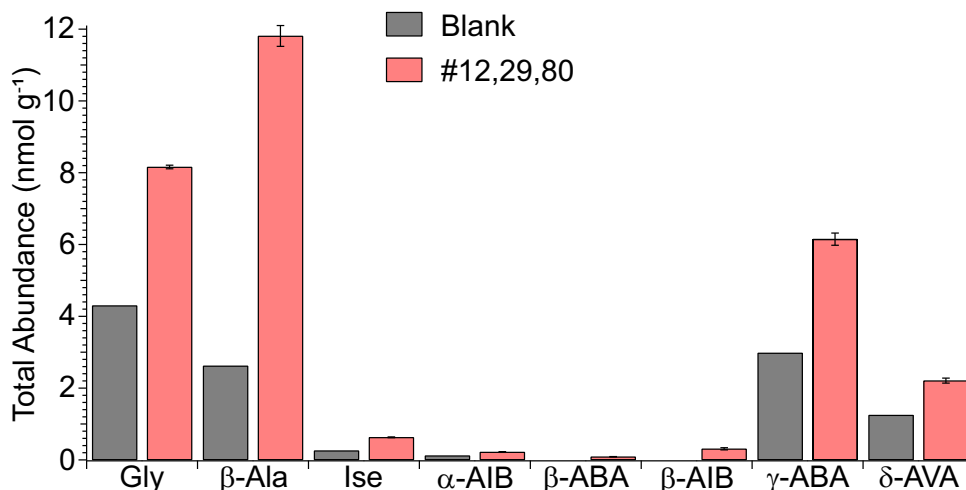


Fig. 3. The comparatively large abundance of β-Ala in the #12,29,80 sample relative to the procedural blank strongly suggests a sample contribution. Blank-uncorrected total abundances of select non-protein amino acids and glycine observed in the #12,29,80 sample compared to their corresponding blank levels. Multiple amino acids were observed above background levels in the #12,29,80 sample with β-Ala being the most abundant. Both β-AIB and β-ABA were identified in the Hayabusa grains, but were not present in the blank. The standard errors reported here were taken from Table 2. Note: Uncertainties of blank abundances are not shown because replicate blank measurements were not made. However, replicate measurements of other laboratory blanks have indicated that background amino acid abundance estimates were not accompanied by large uncertainty estimates.

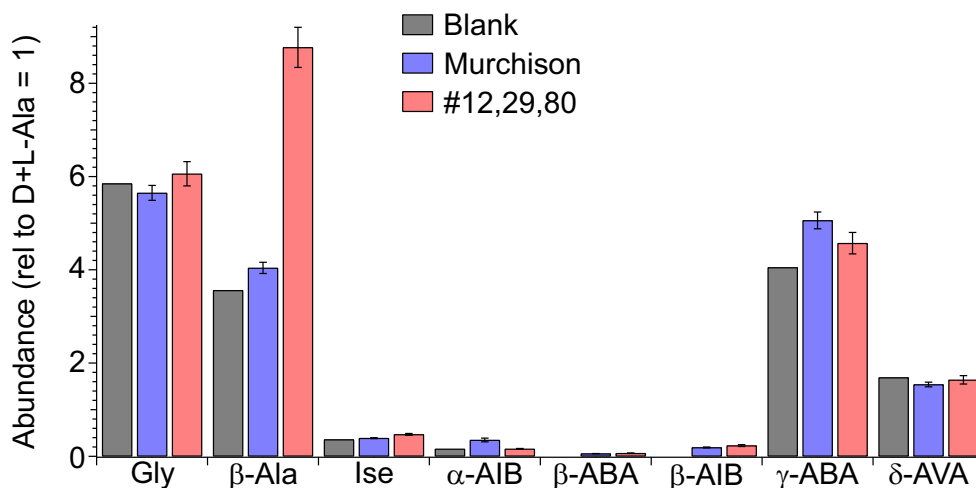


Fig. 4. The enhanced relative abundance of β-Ala in #12,29,80 is distinct from that observed in the blank and therefore supports the hypothesis that a portion of this non-protein amino acid is derived from the sample. Blank-uncorrected relative abundances of select non-protein amino acids and glycine observed for Murchison and #12,29,80. Sample relative abundances are compared to those of the procedural blank to distinguish which analyte relative abundances are inconsistent with background levels, and are therefore likely to have been contributed by the sample. The standard errors reported here were based on the average values and associated standard errors reported in Table 2, and propagated through the appropriate equations. Uncertainties of blank relative abundances are not available because of reasons stated in the Fig. 3 legend.

whereas Naraoka et al. (2012) rinsed the particle surfaces with a small volume ( $\approx 0.6 \mu\text{L}$ ) of 50:50 dichloromethane/methanol for  $\approx 10$  s without applying heat (Naraoka, personal communication). This less aggressive organic extraction approach was chosen because a heated, aqueous extraction protocol would have interfered with planned, downstream mineral analyses by imparting aqueous

weathering to the particles' mineral content (Naraoka et al., 2012). It is plausible the aqueous extraction protocol used in the current study, which entailed a comparatively large extraction volume ( $500 \mu\text{L}$ ) at an elevated temperature ( $100^\circ\text{C}$ ) over a long (24-h) time span (Glavin et al., 1999), provided for more efficacious amino acid extraction.

## Comparison to Other Chondrites

Remote sensing (Abe et al., 2006; Okada et al., 2006) and mineral (Brady & Cherniak, 2010; Huss et al., 2006) data indicate that Itokawa is compositionally similar to LL5 and LL6 ordinary chondrites (OCs). Therefore, comparing published OC amino acid data to those of Hayabusa grains may elucidate if the observed Hayabusa amino acid distribution is consistent with a typical amino acid distribution for representative meteorites. Likely due to the depleted amino acid abundances in OCs, there are few reports of OC amino acids published (Botta et al., 2008; Burton et al., 2011; Chan et al., 2012, 2018; Jenniskens et al., 2014; Martins, Hofmann, et al., 2007). To our knowledge, there are no reports of LL6 OCs and one report with three LL5 OCs: LaPaz Icefield (LAP) 03573, LAP 03624, and LAP 03637 (Botta et al., 2008). These LL5 OCs contained amino acid profiles comprised only of glycine,  $\beta$ -Ala, and  $\gamma$ -ABA at abundances ranging from 0.04 to 0.13 nmol g<sup>-1</sup>. Similar to the LL5s, glycine,  $\beta$ -Ala, and  $\gamma$ -ABA were also the most abundant in #12,29,80 analyzed in the current study. Given the uncertainties in relative amounts of glycine contamination between these LL5s, and the #12,29,80 sample analyzed in the current work, comparing the abundances of  $\beta$ -Ala and  $\gamma$ -ABA among these samples could be a more useful measurement by which to glean information about possible parent body conditions and syntheses that contributed to observed non-protein amino acid abundances, as opposed to comparing abundances of non-protein amino acids to glycine. When performing such a comparison, it was found that the #12,29,80 sample contained a  $\approx 6.2$ –8.0 times greater  $\beta$ -Ala/ $\gamma$ -ABA ratio than the LL5s (Fig. 5). Consequently, the amino acid relative abundances observed in #12,29,80 appear to be distinct from those of LL5 OCs.

In addition to mineralogical similarities with LL5s, it has been reported that Itokawa organic content may have been influenced by the infall of primitive material from CR chondrites (Chan et al., 2021), which contain a greater diversity of amino acids (Glavin et al., 2011) than LL5s. To illustrate, NanoSIMS analysis of the hydrogen, as a proxy for water content, in Itokawa silicates has revealed that Itokawa was likely rehydrated by exogenous delivery of water, perhaps from CR chondrites (Chan et al., 2021). Therefore, it is worth exploring if the  $\beta$ -Ala/ $\gamma$ -ABA ratio of #12,29,80 is similar to that of primitive, carbon-rich CRs to evaluate the likelihood that the amino acids of #12,29,80 may also have been affected by the infall of water-rich CCs. For this purpose, the  $\beta$ -Ala/ $\gamma$ -ABA ratio of the #12,29,80 sample was compared to that of weakly altered (petrologic type >2.5) and more

aqueously altered (petrologic type <2.5) CR chondrites. The weakly altered CR chondrites used for this comparison were CR2.7 Graves Nunataks (GRA) 95229 (Martins, Hofmann, et al., 2007), CR2.7 Miller Range (MIL) 090657 (Aponte et al., 2020), and CR2.8 Queen Alexandria Range (QUE) 99177 and CR2.8 Elephant Moraine (EET) 92042 (Glavin et al., 2011). The more aqueously altered CR chondrites used for this comparison were CR 2.0 Grosvenor Mountains (GRO) 95577 (Glavin et al., 2011) and CR2.4 MIL 090001 (Aponte et al., 2020). The weakly altered CR2s contained  $\beta$ -Ala/ $\gamma$ -ABA ratios of only  $\approx 41$ –64% of that quantitated for #12,29,80, whereas those for more aqueously altered CR2s were  $\approx 82$ –113% of that observed for #12,29,80 (Fig. 5). Furthermore, it can be seen that the total amino acid abundance for #12,29,80 ( $20.3 \pm 0.4$  nmol g<sup>-1</sup>) is concomitantly similar to those ( $\approx 17$ –20 nmol g<sup>-1</sup>) of more aqueously altered CRs, and contrasts with those (up to  $\approx 3000$  nmol g<sup>-1</sup>) of weakly altered CRs (Fig. 5). The combined similarities of the dual amino acid characteristics (i.e.,  $\beta$ -Ala/ $\gamma$ -ABA ratio and total amino acid abundance) between #12,29,80 and more aqueously altered CRs are intriguing to note. Further evaluations of such comparisons during future Itokawa analyses will be important to better assess the plausibility that the amino acid content of Itokawa may have been influenced by exogenous delivery from water-rich chondrites.

Despite similar mineralogical features, differences in amino acid distribution and abundances between these Hayabusa grains and Antarctic LL5 OCs could indicate the Category 3 grains returned by Hayabusa may have originated from another, more carbon-rich parent body. This interpretation is in line with the observation of a 6 m xenolithic black boulder on the surface of Itokawa, which was suggested to be a carbonaceous chondrite originated from an impactor that was 200–800 m in diameter (Chan et al., 2021; Nagaoka et al., 2014). It was also concluded that traces of exogenous material may exist on Itokawa as evidenced by the presence of both primitive and processed organic material within a single Itokawa grain, due to spectral and isotopic similarities to carbon-rich CR carbonaceous chondrites and interplanetary dust particles rather than OCs (Chan et al., 2021). Additionally, a recent SEM-EDX analysis of Itokawa material found evidence of exogenous copper sulfide in the form of a cubanite–chalcopyrite–troilite–pyrrhotite assemblage, the components of which are emblematic of low-temperature, aqueous alteration and more consistent with CI, R, or CK chondrites, as opposed to LL OC-type material akin to that of asteroid Itokawa (Burgess & Stroud, 2021). It is worth noting that DellaGiustina et al. (2021) reported Vestoid-like xenoliths on the surface of asteroid 101955 Bennu

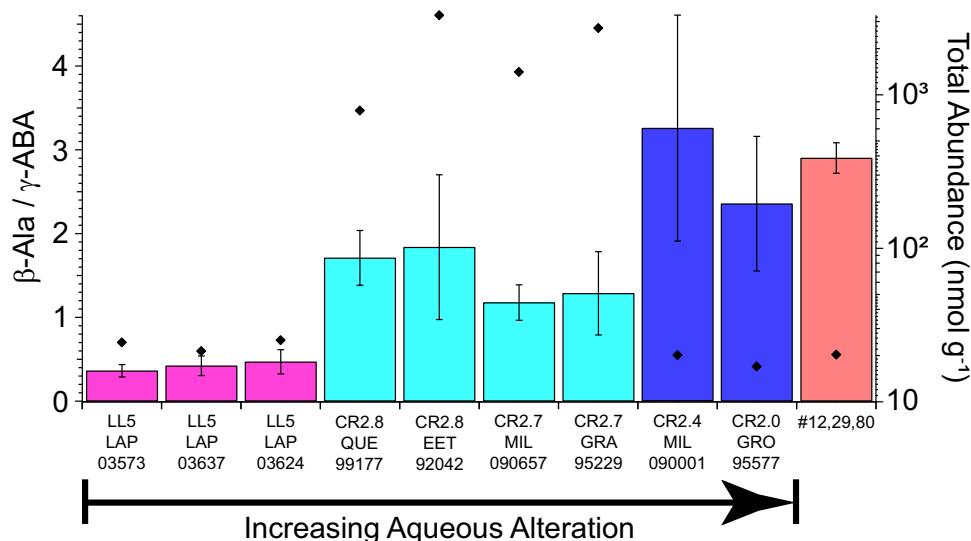


Fig. 5. The  $\beta\text{-Ala}/\gamma\text{-ABA}$  ratio in #12,29,80 is inconsistent with those observed in LL5 OCs and fits some CRs, but not others. The left axis shows the blank-corrected abundance of  $\beta\text{-Ala}$ , relative to  $\gamma\text{-ABA}$ , observed in #12,29,80 and previously analyzed thermally altered LL5 OCs (Botta et al., 2008), more thermally altered CR2s (Aponte et al., 2020; Glavin et al., 2010; Martins, Hofmann, et al., 2007), and more aqueously altered CR2s (Aponte et al., 2020; Glavin et al., 2011). Petrologic subtypes for CR2 chondrites were taken from elsewhere (Harju et al., 2014) for GRO 95577, MIL 090001, GRA 95229, and QUE 99177, and from Aponte et al. (2020) for MIL 090657 and EET 92042. The right axis demonstrates the total amino acid abundances (black diamonds) in the respective samples. The standard error reported here for the  $\beta\text{-Ala}/\gamma\text{-ABA}$  ratio was based on the average values and associated standard errors reported in Table 2, and propagated through the appropriate equations. All other uncertainty estimates shown here were obtained from their respective literature sources.

from in situ observations by the NASA OSIRIS-REx spacecraft. It is possible that such xenolithic material may be found in the OSIRIS-REx sample.

Aside from the possibility of exogenous delivery affecting the organic content of Hayabusa particles, it is possible that the observed amino acid abundances and distributions may be the product of an unusual contamination that is not easily explained by the biology of obvious industrial materials, as the species of primary interest in this study are dissimilar from that which would be expected from biological or industrial contamination. To evaluate such a possibility, comparisons to witness coupons would be beneficial, as has been emphasized previously in the literature (Uesugi et al., 2014; Yabuta et al., 2014). However, Hayabusa lacked flight witness materials; thus, we relied on the distribution and relative abundances of amino acids to discriminate between terrestrial and extraterrestrial origins. The amino acid analyses performed here help to address this need, and the resultant data present evidence to suggest some compounds may have an extraterrestrial origin.

The detection of amino acids in thermally altered asteroid material is nonetheless curious, as thermally altered chondrites were reported to be amino acid poor (Cronin & Moore, 1971, 1976; Glavin et al., 2010). Yet, it is not unfounded for thermally altered material to

contain amino acids. To illustrate, low abundances of amino acids were found in the thermally altered Almahata Sitta ureilite (Burton et al., 2011; Glavin et al., 2010; Herrin et al., 2010; Zolensky et al., 2010), and  $n\text{-}\omega$ -amino acids, including  $\beta\text{-Ala}$ , were abundant in thermally altered CV and CO chondrites (Burton, Elsila, et al., 2012). Comparatively large abundances of  $n\text{-}\omega$ -amino acids like glycine,  $\beta\text{-Ala}$ , and  $\gamma\text{-ABA}$  observed for #12,29,80 are consistent with previous amino acid studies of thermally altered CCs (Burton, Elsila, et al., 2012) and could highlight the potential importance of alternative amino acid formation mechanisms, such as mineral-catalyzed Fischer Tropsch/Haber Bosch-type reactions that may have been prominent in numerous solar system environments (Anders et al., 1973; Levy et al., 1973; Studier et al., 1968). However, the presence of  $\beta\text{-AIB}$  and a high  $\beta\text{-Ala}/\gamma\text{-ABA}$  ratio was not similarly observed in thermally altered CV and CO carbonaceous chondrites, which suggests the involvement of low-temperature aqueous activity may also contribute to amino acid synthesis in Hayabusa material.

### Potential Particle Origins and Associated Implications

Given the extremely small masses of Hayabusa samples available for amino acid analysis, and the sensitive nature of such samples to amino acid

contamination, performing a thorough investigation of particle mineralogy prior to amino acid analysis was not feasible. Doing so would have likely resulted in sample loss or contamination, which would have compromised the scientific integrity of the samples for amino acid analysis. However, there was one particle for which some mineralogical information was available based on initial SEM-EDX analysis, and that was particle #29. Plagioclase was observed in particle #29 upon SEM-EDX analysis performed by the JAXA curation team. Plagioclase is a mineral that has been observed in a variety of CCs and OCs, including CR chondrites (Tenner et al., 2019), CV chondrites (Krot et al., 2002), and type 5 and 6 OCs (Huss et al., 2006; Van Schmus & Wood, 1967). In OCs, plagioclase has been observed as a primary phase (Lewis et al., 2022). Given the ubiquity of plagioclase, the presence of this mineral in particle #29 is not a selective feature for the purpose of constraining a range of possible parent bodies. To investigate the possible origin of the microparticles studied here, namely #29, quantitative SEM-EDX data of these Hayabusa samples was obtained from the JAXA curation team. For particle #29, primary chemical elements that make up plagioclase were observed, such as Na, Al, Si, and O, although these elements tended to be minor components based on quantitative SEM-EDX data. This pattern was similarly observed in the other Hayabusa particles analyzed here, whereby elemental components of the particles that could otherwise help glean possible mineral phase composition within these grains, and in turn aid in assessing the origins of these samples, were relatively low in abundance. In contrast, C was relatively large in abundance in all five Hayabusa grains analyzed here. Given the quantitative SEM-EDX data collected for these particles, it is not possible to adequately constrain the range of parent bodies these grains may have originated from. This matter is complicated by the fact that the grain masses were too small to obtain isotopic data for these samples, which is a very useful analytical tool for determining the origins of samples.

Although the particle origins cannot be deduced based on the SEM-EDX data, it is useful to evaluate how different plausible particle origins would affect the implications of this work, within the context of the amino acid data collected here. The first possible scenario is that the Hayabusa particles analyzed here were collected from the surface of asteroid Itokawa. If so, the amino acid data observed here would indicate that non-protein amino acids, such as  $\beta$ -Ala,  $\beta$ -AIB, and  $\beta$ -ABA, represent extraterrestrial amino acids recovered from the surface of asteroid Itokawa. Furthermore, it is possible that these amino acids may have originated from exogenous material delivered to the Itokawa asteroid surface from a more carbon-rich source. The second possible scenario is

that the particles did not originate from asteroid Itokawa and instead were derived from an unknown terrestrial source. Given the lack of available Hayabusa flight witness materials that experienced the same environments as the samples collected at Itokawa, it is difficult to rule out the possibility that the non-protein amino acids detected in the returned Hayabusa grains were derived from a highly unusual and unknown terrestrial contamination source.

## CONCLUSIONS

The results of this work serve as the first evidence of plausibly extraterrestrial, non-protein amino acids in asteroid material obtained from a sample-return mission. Due to the finite sample masses available for study and the small quantities of amino acids extracted from the grains, compound-specific stable isotopic measurements necessary to make definitive conclusions regarding the specific provenance of these non-protein amino acids and the origins of the measured enantiomeric excesses (Elsila et al., 2009) were not possible. Therefore, isotopic measurements of the amino acid content of Hayabusa material using more sensitive stable isotopic analyses than are currently available, and comparisons with other carbon-rich meteorites and samples returned from Ryugu and Bennu, will be vital to better assess the exact origins of the non-protein amino acids in the Hayabusa grains analyzed here.

Despite similarities between Itokawa and thermally altered LL5 and LL6 OCs (Abe et al., 2006; Brady & Cherniak, 2010; Huss et al., 2006; Okada et al., 2006), the Hayabusa amino acid content observed here was dissimilar to thermally altered OCs (Botta et al., 2008), but preliminarily analogous to more aqueously altered CR2s. This underscores the possibility that materials may have transported between small solar system bodies to contribute to the chemistry of sample-return mission target asteroids (Chan et al., 2021). Through the use of very sensitive and selective analytical techniques, such as the methods described here, discoveries similar to those detailed in this work highlight the power of sample-return missions like Hayabusa2 and OSIRIS-REx to unveil new insights into organic synthesis in the solar system and thereby uncover important implications for the origin of life on Earth and possibly elsewhere.

*Acknowledgments*—The authors are extremely grateful to the JAXA Astromaterials Science Research Group (ASRG) for providing five particles from the Hayabusa mission. We are very thankful to the curators at the JAXA Extraterrestrial Sample Curation Center for providing SEM data for the particles investigated in this

study. The authors also appreciate Dr. Michael Zolensky for providing a Murchison particle for this study. E.T.P. acknowledges funding support from the NASA Emerging Worlds Program (Grant #18-EW18\_2-0121). Q.H.S.C. was supported by a Science and Technology Facilities Council (STFC) rolling grant (ST/P000657/1). E.T.P., D.P.G., and J.P.D. are grateful for funding by a grant from the Simons Foundation (SCOL award 302497 to J.P.D.) and the Goddard Center for Astrobiology, part of the NASA Astrobiology Institute. Q.H.S.C. greatly appreciates JAXA for the extended time provided for the investigation of the Hayabusa particles beyond her maternity leave.

**Data Availability Statement**—The data that support the findings of this study are openly available in the NASA PubSpace archive at <https://www.ncbi.nlm.nih.gov/pmc/funder/nasa/>. The data that support the findings of this study are also available in the supplementary material of this article.

**Editorial Handling**—Dr. Scott Sandford

## REFERENCES

- Abe, M., Takagi, Y., Kitazato, K., Abe, S., Hiroi, T., Vilas, F., Clark, B. E. et al. 2006. Near-Infrared Spectral Results of Asteroid Itokawa from the Hayabusa Spacecraft. *Science* 312: 1334–8.
- Altwegg, K., Balsiger, H., Bar-Nun, A., Berthelier, J.-J., Bieler, A., Bochsler, P., Briois, C. et al. 2016. Prebiotic Chemicals—Amino Acid and Phosphorus—in the Coma of Comet 67P/Churyumov-Gerasimenko. *Science Advances* 2: 1.
- Anders, E., Hayatsu, R., and Studier, M. H. 1973. Organic Compounds in Meteorites. *Science* 182: 781–90.
- Aponte, J. C., Dworkin, J. P., and Elsila, J. E. 2015. Indigenous Aliphatic Amines in the Aqueously Altered Orgueil Meteorite. *Meteoritics & Planetary Science* 50: 1733–49.
- Aponte, J. C., Elsila, J. E., Hein, J. E., Dworkin, J. P., Glavin, D. P., McLain, H. L., Parker, E. T., Cao, T., Berger, E. L., and Burton, A. S. 2020. Analysis of Amino Acids, Hydroxy Acids and Amines in CR Chondrites. *Meteoritics & Planetary Science* 55: 2422–39.
- Botta, O., Martin, Z., Emmenegger, C., Dworkin, J. P., Glavin, D. P., Harvey, R. P., Zenobi, R., Bada, J. L., and Ehrenfreund, P. 2008. Polycyclic Aromatic Hydrocarbons and Amino Acids in Meteorites and Ice Samples from LaPaz Icefield, Antarctica. *Meteoritics & Planetary Science* 43: 1465–80.
- Brady, J. B., and Cherniak, D. J. 2010. Diffusion in Minerals: An Overview of Published Experimental Diffusion Data. In *Diffusion in Minerals and Melts*, edited by Y. Zhang and D. J. Cherniak, 899–920. Chantilly, Virginia: The Mineralogical Society of America.
- Burgess, K. D., and Stroud, R. M. 2021. Exogenous Copper Sulfide in Returned Asteroid Itokawa Regolith Grains Are Likely Relicts of Prior Impacting Body. *Communications Earth & Environment* 2.
- Burton, A. S., Elsila, J. E., Callahan, M. P., Martin, M. G., Glavin, D. P., Johnson, N. M., and Dworkin, J. P. 2012. A Propensity for *n*- $\omega$ -Amino Acids in Thermally Altered Antarctic Meteorites. *Meteoritics & Planetary Science* 47: 374–86.
- Burton, A. S., Glavin, D. P., Callahan, M. P., Dworkin, J. P., Jenniskens, P., and Shaddad, M. H. 2011. Heterogeneous Distributions of Amino Acids Provide Evidence of Multiple Sources Within the Almahata Sitta Parent Body, Asteroid 2008 TC3. *Meteoritics & Planetary Science* 46: 1703–12.
- Burton, A. S., Glavin, D. P., Elsila, J. E., Dworkin, J. P., Jenniskens, P., and Yin, Q.-Z. 2014. The Amino Acid Composition of the Sutter's Mill CM2 Carbonaceous Chondrite. *Meteoritics & Planetary Science* 49: 2074–86.
- Burton, A. S., McLain, H. L., Glavin, D. P., Elsila, J. E., Davidson, J., Miller, K. E., Andronikov, A. V., Lauretta, D., and Dworkin, J. P. 2015. Amino Acid Analyses of R and CK Chondrites. *Meteoritics & Planetary Science* 50: 470–82.
- Burton, A. S., Stern, J. C., Elsila, J. E., Glavin, D. P., and Dworkin, J. P. 2012. Understanding Prebiotic Chemistry Through the Analysis of Extraterrestrial Amino Acids and Nucleobases in Meteorites. *Chemical Society Reviews* 41: 5459–72.
- Chan, Q. H. S., Martins, Z., and Sephton, M. A. 2012. Amino Acid Analyses of Type 3 Chondrites Colony, Ornans, Chainpur, and Bishunpur. *Meteoritics & Planetary Science* 47: 1502–16.
- Chan, Q. H. S., Stephant, A., Franchi, I. A., Zhao, X., Brunetto, R., Kebukawa, Y., Noguchi, T. et al. 2021. Organic Matter and Water from Asteroid Itokawa. *Scientific Reports* 11: 5125.
- Chan, Q. H. S., Zolensky, M. E., Kebukawa, Y., Fries, M., Ito, M., Steele, A., Rahman, Z. et al. 2018. Organic Matter in Extraterrestrial Water-Bearing Salt Crystals. *Science Advances* 4: eaao3521.
- Chyba, C., and Sagan, C. 1992. Endogenous Production, Exogenous Delivery and Impact-Shock Synthesis of Organic Molecules: An Inventory for the Origins of Life. *Nature* 355: 125–32.
- Cronin, J. R., Gandy, W. E., and Pizzarello, S. 1981. Amino-Acids of the Murchison Meteorite: I. Six Carbon Acyclic Primary Alpha-Amino Alkanoic Acids. *Journal of Molecular Evolution* 17: 265–72.
- Cronin, J. R., and Moore, C. B. 1971. Amino Acid Analyses of the Murchison, Murray, and Allende Carbonaceous Chondrites. *Science* 172: 1327–9.
- Cronin, J. R. and Moore, C. B. 1976. Amino Acids of the Nogoya and Mokoia Carbonaceous Chondrites. *Geochimica et Cosmochimica Acta* 40: 853–7.
- Cronin, J. R., and Pizzarello, S. 1983. Amino Acids in Meteorites. *Advances in Space Research* 3: 5–18.
- Cronin, J. R., and Pizzarello, S. 1997. Enantiomeric Excesses in Meteoritic Amino Acids. *Science* 275: 951–5.
- DellaGiustina, D. N., Kaplan, H. H., Simon, A. A., Bottke, W. F., Avdellidou, C., Delbo, M., Ballouz, R.-L. et al. 2021. Exogenic Basalt on Asteroid (101955) Bennu. *Nature Astronomy* 5: 31–8.

- Dworkin, J. P., Adelman, L. A., Ajluni, T., Andronikov, A. V., Aponte, J. C., Bartels, A. E., Beshore, E. et al. 2018. OSIRIS-REx Contamination Control Strategy and Implementation. *Space Science Reviews* 214: 19.
- Ehrenfreund, P., Glavin, D. P., Botta, O., Cooper, G., and Bada, J. L. 2001. Extraterrestrial Amino Acids in Orgueil and Ivuna: Tracing the Parent Body of CI Type Carbonaceous Chondrites. *Proceedings of the National Academy of Sciences* 98: 2138–41.
- Elsila, J. E., Aponte, J. C., Blackmond, D. G., Burton, A. S., Dworkin, J. P., and Glavin, D. P. 2016. Meteoritic Amino Acids: Diversity in Compositions Reflects Parent Body Histories. *ACS Central Science* 2: 370–9.
- Elsila, J. E., Glavin, D. P., and Dworkin, J. P. 2009. Cometary Glycine Detected in Samples Returned by Stardust. *Meteoritics & Planetary Science* 44: 1323–30.
- Elsila, J. E., Johnson, N. M., Glavin, D. P., Aponte, J. C., and Dworkin, J. P. 2021. Amino Acid Abundances and Compositions in Iron and Stony-Iron Meteorites. *Meteoritics & Planetary Science* 56: 586–600.
- Engel, M., and Macko, S. 1997. Isotopic Evidence for Extraterrestrial Non-Racemic Amino Acids in the Murchison Meteorite. *Nature* 389: 265–8.
- Engel, M. H., and Nagy, B. 1982. Distribution and Enantiomeric Composition of Amino Acids in the Murchison Meteorite. *Nature* 296: 837–40.
- Glavin, D. P., Aubrey, A. D., Callahan, M. P., Dworkin, J. P., Elsila, J. E., Parker, E. T., Bada, J. L., Jenniskens, P., and Shaddad, M. H. 2010. Extraterrestrial Amino Acids in the Almahata Sitta Meteorite. *Meteoritics & Planetary Science* 45: 1695–709.
- Glavin, D. P., Bada, J. L., Brinton, K. L. F., and McDonald, G. D. 1999. Amino Acids in the Martian Meteorite Nakhla. *Proceedings of the National Academy of Sciences* 96: 8835–8.
- Glavin, D. P., Burton, A. S., Elsila, J. E., Aponte, J. C., and Dworkin, J. P. 2020. The Search for Chiral Asymmetry As a Potential Biosignature in Our Solar System. *Chemical Reviews* 120: 4660–89.
- Glavin, D. P., Callahan, M. P., Dworkin, J. P., and Elsila, J. E. 2011. The Effects of Parent Body Processes on Amino Acids in Carbonaceous Chondrites. *Meteoritics & Planetary Science* 45: 1948–72.
- Glavin, D. P., and Dworkin, J. P. 2009. Enrichment of the Amino Acid L-Isovaline by Aqueous Alteration on CI and CM Meteorite Parent Bodies. *Proceedings of the National Academy of Sciences* 106: 5487–92.
- Glavin, D. P., Dworkin, J. P., Aubrey, A., Botta, O., Doty, J. H., Martins, Z., and Bada, J. L. 2006. Amino Acid Analyses of Antarctic CM2 Meteorites Using Liquid Chromatography-Time of Flight-Mass Spectrometry. *Meteoritics & Planetary Science* 41: 889–902.
- Glavin, D. P., Elsila, J. E., McLain, H. L., Aponte, J. C., Parker, E. T., Dworkin, J. P., Hill, D. H., Connolly Jr., H. C., and Lauretta, D. S. 2021. Extraterrestrial Amino Acids and L-Enantiomeric Excesses in the CM2 Carbonaceous Chondrites Aguas Zarcas and Murchison. *Meteoritics & Planetary Science* 56: 148–73.
- Hamase, K., Nakauchi, Y., Miyoshi, Y., Koga, R., Kusano, N., Onigahara, H., Naraoka, H. et al. 2014. Enantioselective Determination of Extraterrestrial Amino Acids Using a Two-Dimensional Chiral High-Performance Liquid Chromatographic System. *Chromatography* 35: 103–10.
- Harju, E. R., Rubin, A. E., Ahn, I., Choi, B.-G., Ziegler, K., and Wasson, J. T. 2014. Progressive Aqueous Alteration of CR Carbonaceous Chondrites. *Geochimica et Cosmochimica Acta* 139: 267–92.
- Herrin, J. S., Zolensky, M. E., Ito, M., Le, L., Mittlefehldt, D. W., Jenniskens, P., Ross, A. J., and Shaddad, M. H. 2010. Thermal and Fragmentation History of Ureilitic Asteroids: Insights from the Almahata Sitta Fall. *Meteoritics & Planetary Science* 45: 1789–803.
- Huss, G. R., Rubin, A. E., and Grossman, J. N. 2006. Thermal Metamorphism in Chondrites. In *Meteorites and the Early Solar System II*, edited by D. S. Lauretta and H. Y. McSween Jr., 567–86. Tucson, Arizona: The University of Arizona Press.
- Ito, M., Uesugi, M., Naraoka, H., Yabuta, H., Kitajima, F., Mita, H., Takano, Y. et al. 2014. H, C, and N Isotopic Compositions of Hayabusa Category 3 Organic Samples. *Earth, Planets and Space* 66: 102.
- Jenniskens, P., Rubin, A. E., Yin, Q.-Z., Sears, D. W. G., Sandford, S. A., Zolensky, M. E., Krot, A. N. et al. 2014. Fall, Recovery, and Characterization of the Novato L6 Chondrite Breccia. *Meteoritics & Planetary Science* 49: 1388–425.
- Kitajima, F., Uesugi, M., Karouji, Y., Ishibashi, Y., Yada, T., Naraka, H., Abe, M. et al. 2015. A Micro-Raman and Infrared Study of Several Hayabusa Category 3 (Organic) Particles. *Earth, Planets and Space* 67: 20.
- Koga, T., and Naraoka, H. 2017. A New Family of Extraterrestrial Amino Acids in the Murchison Meteorite. *Scientific Reports* 7: 636.
- Krot, A. N., Hutcheon, I. D., and Keil, K. 2002. Plagioclase-Rich Chondrules in the Reduced CV Chondrites: Evidence for Complex Formation History and Genetic Links Between Calcium-Aluminum-Rich Inclusions and Ferromagnesian Chondrules. *Meteoritics & Planetary Science* 37: 155–182.
- Kvenvolden, K. A., Glavin, D. P., and Bada, J. L. 2000. Extraterrestrial Amino Acids in the Murchison Meteorite: Re-Evaluation After Thirty Years. In *Perspectives in Amino Acid and Protein Geochemistry*, edited by G. A. Goodfriend, M. J. Collins, M. L. Fogel, S. A. Macko, and J. F. Wehmiller, 7–14. New York: Oxford University Press Inc.
- Kvenvolden, K., Lawless, J., Pering, K., Peterson, E., Flores, J., Ponnampuruma, C., Kaplan, I. R., and Moore, C. 1970. Evidence for Extraterrestrial Amino-Acids and Hydrocarbons in the Murchison Meteorite. *Nature* 228: 923–6.
- Levy, R. L., Grayson, M. A., and Wolf, C. J. 1973. The Organic Analysis of the Murchison Meteorite. *Geochimica et Cosmochimica Acta* 37: 467–83.
- Lewis, J. A., Jones, R. H., and Brearley, A. J. 2022. Plagioclase Alteration and Equilibration in Ordinary Chondrites: Metasomatism During Thermal Metamorphism. *Geochimica et Cosmochimica Acta* 316: 201–29.
- Lie, Y., Farmer, T. J., and Macquarrie, D. J. 2018. Facile and Rapid Decarboxylation of Glutamic Acid to  $\gamma$ -Aminobutyric Acid via Microwave-Assisted Reaction: Towards Valorisation of Waste Gluten. *Journal of Cleaner Production* 205: 1102–13.
- Macke, R. J., Consolmagno, G. J., and Britt, D. T. 2011. Density, Porosity, and Magnetic Susceptibility of Carbonaceous Chondrites. *Meteoritics & Planetary Science* 46: 1842–62.
- Martins, Z., Alexander, C. M. O'D., Orzechowska, G. E., Fogel, M. L., and Ehrenfreund, P. 2007. Indigenous

- Amino Acids in Primitive CR Meteorites. *Meteoritics & Planetary Science* 42: 2125–36.
- Martins, Z., Hofmann, B. A., Gnoss, E., Greenwood, R. C., Verchovsky, A., Franchi, I. A., Jull, A. J. T. et al. 2007. Amino Acid Composition, Petrology, Geochemistry,  $^{14}\text{C}$  Terrestrial Age and Oxygen Isotopes of the Sh $\ddot{u}$ r 033 CR Chondrite. *Meteoritics & Planetary Science* 42: 1581–95.
- Messenger, S. 2000. Identification of Molecular-Cloud Material in Interplanetary Dust Particles. *Nature* 404: 968–71.
- Nagaoka, H., Takasawa, S., Nakamura, A. M., and Sengen, K. 2014. Degree of Impactor Fragmentation Under Collision with a Regolith Surface—Laboratory Impact Experiments of Rock Projectiles. *Meteoritics & Planetary Science* 49: 69–79.
- Naraoka, H., Aoki, D., Fukushima, K., Uesugi, M., Ito, M., Kitajima, F., Mita, H. et al. 2015. ToF-SIMS Analysis of Carbonaceous Particles in the Sample Catcher of the Hayabusa Spacecraft. *Earth, Planets and Space* 67: 67.
- Naraoka, H., Mita, H., Hamase, K., Mita, M., Yabuta, H., Saito, K., Fukushima, K. et al. 2012. Preliminary Organic Compound Analysis of Microparticles Returned from Asteroid 25143 Itokawa by the Hayabusa Mission. *Geochimical Journal* 46: 61–72.
- Okada, T., Shirai, K., Yamamoto, Y., Arai, T., Ogawa, K., Hosono, K., and Kato, M. 2006. X-Ray Fluorescence Spectrometry of Asteroid Itokawa by Hayabusa. *Science* 312: 1338–41.
- Peltzer, E. T., Bada, J. L., Schlesinger, G., and Miller, S. L. 1984. The Chemical Conditions on the Parent Body of the Murchison Meteorite: Some Conclusions Based on Amino, Hydroxy and Dicarboxylic Acids. *Advances in Space Research* 4: 69–74.
- Peterson, E., Horz, F., and Chang, S. 1997. Modification of Amino Acids at Shock Pressures of 3.5 to 32 GPa. *Geochimica et Cosmochimica Acta* 61: 3937–50.
- Pizzarello, S., and Cronin, J. R. 2000. Non-Racemic Amino Acids in the Murchison and Murray Meteorites. *Geochimica et Cosmochimica Acta* 64: 329–38.
- Pizzarello, S., Huang, Y., and Fuller, M. 2004. The Carbon Isotopic Distribution of Murchison Amino Acids. *Geochimica et Cosmochimica Acta* 68: 4963–9.
- Pizzarello, S., Zolensky, M., and Turk, K. A. 2003. Nonracemic Isovaline in the Murchison Meteorite: Chiral Distribution and Mineral Association. *Geochimica et Cosmochimica Acta* 67: 1589–95.
- Ratcliff Jr., M. A., Medley, E. E., and Simmonds, P. G. 1974. Pyrolysis of Amino Acids. Mechanistic Considerations. *The Journal of Organic Chemistry* 39: 1481–90.
- Simkus, D. N., Aponte, J. C., Elsila, J. E., Parker, E. T., Glavin, D. P., and Dworkin, J. P. 2019. Methodologies for Analyzing Soluble Organic Compounds in Extraterrestrial Samples: Amino Acids, Amines, Monocarboxylic Acids, Aldehydes, and Ketones. *Life* 9: 47.
- Studier, M. H., Hayatsu, R., and Anders, E. 1968. Origin of Organic Matter in Early Solar System—I. Hydrocarbons. *Geochimica et Cosmochimica Acta* 32: 151–73.
- Tenner, T. J., Nakashima, D., Ushikubo, T., Tomioka, N., Kimura, M., Weisberg, M. K., and Kita, N. K. 2019. Extended Chondrule Formation Intervals in Distinct Physicochemical Environments: Evidence from Al-Mg Isotope Systematics of CR Chondrite Chondrules with Unaltered Plagioclase. *Geochimica et Cosmochimica Acta* 260: 133–60.
- Uesugi, M., Naraoka, H., Ito, M., Yabuta, H., Kitajima, F., Takano, Y., Mita, H. et al. 2014. Sequential Analysis of Carbonaceous Materials in Hayabusa-Returned Samples for the Determination of Their Origin. *Earth, Planets and Space* 66: 102.
- Vallentyne, J. R. 1964. Biogeochemistry of Organic Matter—II Thermal Reaction Kinetics and Transformation Products of Amino Compounds. *Geochimica et Cosmochimica Acta* 28: 157–88.
- Van Schmus, W. R., and Wood, J. A. 1967. A Chemical-Petrologic Classification for the Chondritic Meteorites. *Geochimica et Cosmochimica Acta* 31: 747–54.
- Weiss, I. M., Muth, C., Drumm, R., and Kirchner, H. O. K. 2018. Thermal Decomposition of the Amino Acids Glycine, Cysteine, Aspartic Acid, Asparagine, Glutamic Acid, Glutamine, Arginine and Histidine. *BMC Biophysics* 11: 2.
- Wilkison, S. L., and Robinson, M. S. 2000. Bulk Density of Ordinary Chondrite Meteorites and Implications for Asteroidal Internal Structure. *Meteoritics & Planetary Science* 35: 1203–13.
- Yabuta, H., Noguchi, T., Itoh, S., Sakamoto, N., Hashiguchi, M., Abe, K., Tsujimoto, S. et al. 2013. Evidence of Minimum Aqueous Alteration in Rock-Ice Body: Update of Organic Chemistry and Mineralogy of Ultracarbonaceous Antarctic Micrometeorite (Abstract #2335). 44th Lunar and Planetary Science Conference. CD-ROM.
- Yabuta, H., Uesugi, M., Naraoka, H., Ito, M., Kilcoyne, A. L. D., Sandford, S. A., Kitajima, F. et al. 2014. X-Ray Absorption Near Edge Structure Spectroscopic Study of Hayabusa Category 3 Carbonaceous Particles. *Earth, Planets and Space* 66: 156.
- Yada, T., Fujimura, A., Abe, M., Nakamura, T., Noguchi, T., Okazaki, R., Nagao, K. et al. 2014. Hayabusa-Returned Sample Curation in the Planetary Material Sample Curation Facility of JAXA. *Meteoritics & Planetary Science* 49: 135–53.
- Zolensky, M., Herrin, J., Mikouchi, T., Ohsumi, K., Friedrich, J., Steele, A., Rumble, D. et al. 2010. Mineralogy and Petrography of the Almahata Sitta Ureilite. *Meteoritics & Planetary Science* 45: 1618–37.

## SUPPORTING INFORMATION

Additional supporting information may be found in the online version of this article.

**Fig. S1.** Analyses of C<sub>2</sub>–C<sub>4</sub> amino acids in analytical reagents prior to their use during sample preparation and analysis indicated only small amounts of Gly and L-Ala were detected in select reagents. The 34- to 46-

min LC/ToF-MS chromatograms of *m/z* 337.0858 for Gly in a mixed amino acid standard (A), ultrapure water intended for use during hot water extraction (B), tdHCl intended for use during acid vapor hydrolysis (C), and a water blank derivatized as described in §1.2 of the supporting information to examine potential uncertainty in amino acid measurements introduced during derivatization (D). The 40- to 55-min LC/ToF-



MS chromatograms of  $m/z$  351.1015 for  $\beta$ -Ala and D,L-Ala in a mixed amino acid standard (E), ultrapure water intended for use during hot water extraction (F), tdHCl intended for use during acid vapor hydrolysis (G), and a water blank derivatized as described in §1.2 of the supporting information (H). The 45- to 70-min LC/ToF-MS chromatograms of  $m/z$  365.1171 for C<sub>4</sub> non-protein amino acids in a mixed amino acid standard (I), ultrapure water intended for use during hot water extraction (J), tdHCl intended for use during acid vapor hydrolysis (K), and a water blank derivatized as described in §1.2 of the supporting information (L). The asterisk in trace (E) represents an unidentified peak that did not interfere with target analyte detection. Here, analyte identification follows that described in Table S2. Note: the D-Ala peak in trace (E) is less intense than the corresponding L-Ala peak because of ion suppression experienced due to interference from the coelution of unreacted derivatization agent. Intensities of all reagent mass chromatograms are normalized to those of their corresponding mixed amino acid standard mass chromatograms.

**Fig. S2.** The Hayabusa particles analyzed here were carbon-rich grains. Prior to amino acid analysis, the Hayabusa particles were analyzed by SEM-EDX, which revealed evidence of organic signatures, such as elemental C, N, and O. SEM-EDX analyses showed elemental compositions for particles #12 (A), #29 (B), #52 (C), #78 (D), and #80 (E), consistent with those described at the JAXA Hayabusa curation facility website (<https://curation.isas.jaxa.jp/curation/hayabusa/>, accessed 22 February 2022). The spectra shown here are the result of spot analyses. The particles displayed some heterogeneity, but the SEM spectra are representative of the C-rich areas of each grain.

**Fig. S3.** Schematic of data analysis method employed to determine that strong evidence existed to suggest a portion of the abundance of a detected amino acid was indigenous to the sample. The highlighted route in red exhibits the path used to determine that quantitated sample amino acid abundances were likely to be at least partially indigenous to the sample, as opposed to being solely a product of contamination. If the evaluation criteria of fewer than all five steps of this data analysis method were satisfied by a given amino acid, it was determined that there was insufficient evidence to suggest the amino acid in question was at least partially indigenous to the sample.

**Fig. S4.** A total of 36 analytes were analyzed for by the analytical technique employed here. The 10- to 100-min region of a fluorescence chromatogram of a mixed amino acid standard. Select amino acids experienced some chromatographic coelution; however, all amino

acids that were not fully resolved by chromatography, alone, were fully resolved by a combination of chromatography and accurate mass analysis, except for the enantiomers of  $\alpha$ -ABA and Nva. Analyte identifications shown here are consistent with those detailed in Table S2, and are as follows: 1 = D-Asp, 2 = L-Asp, 3 = L-Glu, 4 = D-Glu, 5 = D-Ser, 6 = L-Ser, 7 = D-Ise, 8 = D-Thr, 9 = L-Ise, 10 = L-Thr, 11 = Gly, 12 =  $\beta$ -Ala, 13 =  $\gamma$ -ABA, 14 = D- $\beta$ -AIB, 15 = L- $\beta$ -AIB, 16 = D-Ala, 17 = L-Ala, 18 = D- $\beta$ -ABA, 19 = L- $\beta$ -ABA, 20 =  $\delta$ -AVA, 21 =  $\alpha$ -AIB, 22 = D,L- $\alpha$ -ABA, 23 = D-Iva, 24 = S-3-APA, 25 =  $\epsilon$ -ACA, 26 = L-Iva, 27 = R-3-APA, 28 = L-Val, 29 = D-Val, 30 = D-Nva, 31 = L-Nva, 32 = L-Ile, 33 = 8-AOA, 34 = D-Ile, 35 = D-Leu, 36 = L-Leu.

**Fig. S5.** The samples and procedural blank were found to be contaminated with  $\epsilon$ -ACA; however, contamination did not prevent the detection of other amino acids. The 10- to 100-min fluorescence chromatograms of a mixed amino acid standard (A and E), a blank (B and F), Murchison and #52 (C and G, respectively), and #12,29,80 and #78 (D and H, respectively). The most prominent analyte observed in the blank and samples was the background contaminant,  $\epsilon$ -ACA (peak 25). However, the presence of this background contaminant did not prevent the detection of other species that were present at relatively small abundances, such as glycine,  $\beta$ -Ala, and  $\gamma$ -ABA. Analyte identifications shown here are consistent with those detailed in Table S2.

**Fig. S6.** Accurate mass chromatograms indicated detection of  $\beta$ -Ala in Murchison and #12,29,80. Analysis of  $\beta$ -Ala in a mixed amino acid standard, the procedural blank, Murchison, and #12,29,80, as depicted by their respective 42- to 50-min accurate mass chromatograms for the  $m/z$  351.1015  $\pm$  10 ppm trace. Analyte identifications are consistent with those detailed in Table S2. The  $\beta$ -Ala peak in #12,29,80 was significantly larger than that in the procedural blank, suggesting that while some of the  $\beta$ -Ala signal detected in #12,29,80 is contributed by the blank, a large portion of the  $\beta$ -Ala signal in #12,29,80 may be indigenous to the sample.

**Fig. S7.** Accurate mass chromatograms indicated detection of  $\beta$ -AIB and  $\beta$ -ABA in samples analyzed here. Analyses of C<sub>4</sub> non-protein amino acids in a mixed amino acid standard, the procedural blank, Murchison, #12,29,80, #52, and #78, as depicted by their respective 50- to 72-min accurate mass chromatograms for the  $m/z$  365.1171  $\pm$  10 ppm traces. Analyte identifications are consistent with those detailed in Table S2 and are as follows: 13 =  $\gamma$ -ABA, 14 = D- $\beta$ -AIB, 15 = L- $\beta$ -AIB, 18 = D- $\beta$ -ABA, 19 = L- $\beta$ -ABA, 21 =  $\alpha$ -AIB, 22 = D,L- $\alpha$ -ABA. Small quantities of  $\beta$ -AIB were detected in all samples and low abundances of  $\beta$ -ABA were detected

primarily in Murchison and #12,29,80. Note: retention times of analytes were shifted for #78 and #52 because these two samples were analyzed on a different day than were the Murchison and #12,29,80 samples.

**Fig. S8.** Several species were detected above blank levels in the Murchison sample. Blank-uncorrected total abundances of select C<sub>3</sub> to C<sub>5</sub> non-protein amino acids and glycine observed in Murchison compared to corresponding blank levels. Several non-protein amino acids and glycine were observed in Murchison at abundances greater than blank levels. The standard errors reported here were taken from Table 2 of the main manuscript. Note: uncertainties of blank abundances are not shown because replicate blank measurements were not made. However, replicate measurements of other laboratory blanks have indicated that background amino acid abundance estimates are not accompanied by large uncertainty estimates.

**Fig. S9.** Particle #52 was depleted in amino acids relative to blank levels. Blank-uncorrected total abundances of select C<sub>3</sub> to C<sub>5</sub> non-protein amino acids and glycine observed in #52 compared to corresponding blank levels. The non-protein amino acids,  $\beta$ -ABA and  $\beta$ -AIB were detected at low abundances compared to blank levels, while the other amino acids were depleted relative to blank levels. The standard errors reported here were taken from Table 2 of the main manuscript. Uncertainties of blank relative abundances were not available because of reasons stated in the Fig. S8 legend.

**Fig. S10.** Particle #78, like #52, was depleted in amino acids relative to blank levels. Blank-uncorrected total abundances of select C<sub>3</sub> to C<sub>5</sub> non-protein amino acids and glycine observed in #78 compared to corresponding blank levels. The nonprotein amino acid,  $\beta$ -AIB was detected at low abundances, but the other species depicted here did not exceed blank levels. The standard errors reported here were taken from Table 2 of the main manuscript. Uncertainties of blank relative abundances were not available because of reasons stated in the Fig. S8 legend.

**Fig. S11.** Comparisons of amino acid abundances in samples relative to blank levels indicated that select species in Murchison and #12,29,80 were present at abundances distinct from blank levels and thus may be native to their respective samples. Blank-uncorrected abundances, relative to their corresponding blank levels, of select C<sub>3</sub> to C<sub>5</sub> non-protein amino acids and glycine observed in the samples analyzed here. The sample species whose abundances were most strikingly different from blank levels were  $\beta$ -Ala, Ise, and  $\gamma$ -ABA in #12,29,80, and  $\alpha$ -AIB and  $\gamma$ -ABA in Murchison. The non-protein amino acids,  $\beta$ -AIB and  $\beta$ -ABA were not included in this comparison because these species were below detection limits in the procedural blank. Note:

uncertainty estimates were not provided for amino acid abundances relative to blank levels because of reasons stated in the Fig. S8 legend. Therefore, blank uncertainty estimates were not available to propagate through the appropriate equations.

**Fig. S12.** The enlarged relative abundance of  $\beta$ -Ala in #12,29,80 supports the hypothesis that a portion of this non-protein amino acid's abundance was likely to be native to the grains analyzed. Blank-uncorrected abundances, relative to glycine, of select non-protein amino acids and alanine observed in the Murchison and #12,29,80 samples studied here. Sample relative abundances were compared to those of the procedural blank to distinguish which sample amino acid relative abundances exceeded those of blank levels beyond sample measurement analytical errors, and were therefore likely to have been contributed by the sample. The standard errors reported here were based on the average values and associated standard errors reported in Table 2 of the main manuscript, and propagated through the appropriate equations. Uncertainties of blank relative abundances were not available because of reasons stated in the Fig. S8 legend.

**Fig. S13.** The pronounced relative abundance of  $\beta$ -Ala in #12,29,80 suggested this non-protein amino acid's abundance was easily distinguishable from blank levels and thus likely to have been native to the sample. Blank-uncorrected abundances, relative to L-Ala, of select non-protein amino acids and glycine observed in Murchison and #12,29,80. Sample relative abundances were compared to those of the procedural blank to assess the likelihood these sample amino acids may have been contributed by their respective grains. The standard errors reported here were based on the average values and associated standard errors reported in Table 2 of the main manuscript, and propagated through the appropriate equations. Uncertainties of blank relative abundances were not available because of reasons stated in the Fig. S8 legend.

**Fig. S14.** The abundance, relative to D-Ala, of  $\beta$ -Ala for #12,29,80 remained consistently large, but that of  $\gamma$ -ABA dropped in contrast to previous relative abundance profiles observed for  $\gamma$ -ABA. Blank-uncorrected abundances, relative to D-Ala, of select non-protein amino acids and glycine observed in Murchison and #12,29,80, compared to blank levels. While the relative abundance profiles of  $\beta$ -Ala for #12,29,80,  $\alpha$ -AIB for Murchison, and  $\beta$ -ABA and  $\beta$ -AIB for both Murchison and #12,29,80 remained consistent with previous relative abundance profiles (Fig. S12, S13) and thus suggested these species were attributable to their respective samples, it is noteworthy that the relative abundance profile of  $\gamma$ -ABA for #12,29,80 was strikingly distinct from the previously observed relative abundance profiles of  $\gamma$ -ABA

for #12,29,80 (Fig. S12, S13). This contrast indicated that the abundance of  $\gamma$ -ABA for #12,29,80 may likely have been more heavily attributable to the blank than the sample, itself. The standard errors reported here were based on the average values and associated standard errors reported in Table 2 of the main manuscript, and propagated through the appropriate equations. Uncertainties of blank relative abundances were not available because of reasons stated in the Fig. S8 legend.

**Table S1.** Post-hydrolysis reconstitution volumes and derivatization volumes of the gold foil procedural blank, the Hayabusa particles, and the Murchison sample extracted for amino acid analyses in this study.

**Table S2.** Detection metrics observed when analyzing a mixed amino acid standard using the analytical technique described in this study.

**Table S3.** Detection metrics of select non-protein amino acids and glycine in the samples studied here. Mass errors were calculated as described for Table S2.

**Table S4.** Summary of the D/L ratios and  $L_{ee}$  measured for select amino acids in the acid-hydrolyzed hot water extracts of the CM2 Murchison grain and Hayabusa particles analyzed here.

**Data S1.** This dataset provides the raw data used to generate the fluorescence chromatograms of Fig. 2 of the main manuscript, which shows the 11- to 63-min regions of the fluorescence chromatograms for a mixed amino acid standard, the procedural blank, Murchison, and #12,29,80.

**Data S2.** This dataset provides raw data to generate the mass chromatograms shown in Fig. S1 of the supporting information, which illustrates background amino acid abundances present in the analytical reagents used during sample preparation and analysis. In particular, the ultrapure water used for hot water extraction, the tDHCl used for acid vapor hydrolysis, and the derivatization materials were all evaluated for cleanliness prior to exposing samples to these reagents. This test provided a baseline appraisal of amino acid abundance uncertainties contributed by sample preparation and derivatization steps. This test revealed only small amounts of Gly and L-Ala were detected in select reagents used, indicating it was unlikely that large uncertainties in the observed amino acid abundances, namely  $\beta$ -Ala, were introduced by the wet chemical procedures (i.e., extraction, hydrolysis, and derivatization) used here.

**Data S3.** This dataset provides the raw data used to generate the SEM-EDX spectra shown in Fig. S2 of the supporting information. Fig. S2 of the supporting information shows that the Hayabusa particles analyzed here were carbon-rich and contained such organic signatures as elemental C, N, and O.

**Data S4.** This dataset provides the raw data used to generate the fluorescence chromatogram shown in Fig. S4 of the supporting information. Fig. S4 of the supporting information shows the 10- to 100-min region of a fluorescence chromatogram of a mixed amino acid standard. Select amino acids experienced some chromatographic coelution; however, all amino acids that were not fully resolved by chromatography, alone, were fully resolved by a combination of chromatography and accurate mass analysis, except for the enantiomers of  $\alpha$ -ABA and Nva.

**Data S5.** This dataset provides the raw data used to generate the fluorescence chromatograms in Fig. S5 of the supporting information, which show the 10- to 100-min chromatograms of a mixed amino acid standard (A and E), a blank (B and F), Murchison and #52 (C and G, respectively), and #12,29,80 and #78 (D and H, respectively). The most prominent analyte observed was the background contaminant,  $\epsilon$ -ACA (peak 25). However, the presence of this background contaminant did not prevent the detection of other species present at small abundances (e.g., Gly,  $\beta$ -Ala, and  $\gamma$ -ABA).

**Data S6.** This dataset provides the raw data used to generate the accurate mass chromatograms shown in Fig. S6 of the supporting information. Fig. S6 of the supporting information shows data from the analysis of  $\beta$ -Ala in a mixed amino acid standard, the procedural blank, Murchison, and #12,29,80, as depicted by their respective 42- to 50-min accurate mass chromatograms for the  $m/z$   $351.1015 \pm 10$  ppm trace. The  $\beta$ -Ala peak in #12,29,80 is significantly larger than that in the procedural blank, suggesting that while some of the  $\beta$ -Ala signal detected in #12,29,80 is contributed by the blank, a large portion of the  $\beta$ -Ala signal in #12,29,80 may be indigenous to the sample.

**Data S7.** This dataset provides the raw data used to generate the accurate mass chromatograms shown in Fig. S7 of the supporting information. Fig. S7 of the supporting information shows data from the analysis of C<sub>4</sub> non-protein amino acids in a mixed amino acid standard, the procedural blank, Murchison, #12,29,80, #52, and #78, as depicted by their respective 50- to 72-min accurate mass chromatograms for the  $m/z$   $365.1171 \pm 10$  ppm trace. Small quantities of  $\beta$ -AIB were detected in all samples, and low abundances of  $\beta$ -ABA were detected primarily in Murchison and #12,29,80. Note: retention times of analytes were shifted for #78 and #52 because these two samples were analyzed on a different day than were the Murchison and #12,29,80 samples.